The WNT1 induced signalling protein 1 is a novel mediator of impaired epithelial-mesenchymal interactions in lung fibrosis

Inaugural Dissertation

submitted to the Faculty of Medicine

in partial fulfillment of the requirements

for the PhD-Degree

of the Faculties of Veterinary Medicine and Medicine

of the Justus Liebig University Giessen

by

Dr. med. Melanie Königshofff

from

Wilhelmshaven

Giessen 2009

From the Department of Internal Medicine II
of the Faculty of Medicine of the Justus Liebig University Giessen
Director: Prof. Dr. W. Seeger

Prof. Dr. Werner Seeger (Supervisior)
Priv.-Doz. Dr. Antje Prasse
Prof. Dr. Martin Diener
Prof. Dr. Ritva Tikkanen

Date of Doctoral Defense: August 14, 2009

TABLE OF CONTENT

SUMMARY

Idiopathic pulmonary fibrosis (IPF) is characterized by distorted lung architecture and loss of respiratory function. Enhanced (myo)-fibroblast activation, ECM deposition, and alveolar epithelial type II (ATII) cell dysfunction contribute to IPF pathogenesis. However, the molecular pathways linking ATII cell dysfunction with the development of fibrosis are poorly understood. Here, we demonstrate, in a mouse model of pulmonary fibrosis, increased proliferation and altered expression of components of the WNT/β-catenin signalling pathway in ATII cells. Further analysis revealed that expression of WNT1-inducible signalling protein–1 (WISP1), which is encoded by a WNT target gene, was increased in ATII cells in both a mouse model of pulmonary fibrosis and patients with IPF. Treatment of mouse primary ATII cells with recombinant WISP1 led to increased proliferation and epithelial-mesenchymal transition (EMT), while treatment of human lung fibroblasts with recombinant WISP1 enhanced deposition of ECM components. In the mouse model of pulmonary fibrosis, neutralizing mAbs specific for WISP1 reduced the expression of genes characteristic of fibrosis and reversed the expression of genes associated with EMT. More importantly, these changes in gene expression were associated with marked attenuation of lung fibrosis, including decreased collagen deposition and improved lung function and survival. Our study thus identifies WISP1 as a key regulator of ATII cell hyperplasia and impaired epithelial-mesenchymal interaction as well as a potential therapeutic target for attenuation of pulmonary fibrosis.

ZUSAMMENFASSUNG

Fibrosierende Lungenerkrankungen sind durch eine vermehrte Ansammlung extrazellulärer Matrix und Proliferation der interstiziellen Fibroblasten charakterisiert. Dies führt zu einem kompletten Gewebsumbau der Lunge und einem funktionellem Verlust an Alveolarraum. Im Verlauf der Erkrankung führen wiederholte epitheliale Schädigungen mit versuchten Reparaturvorgängen zu einer Veränderung des Genexpressionsprofils der alveolären Epithelzellen Typ II (ATII-Zellen), was zu einer weiteren Aktivierung der Fibroblasten zu Myofibroblasten führt. In dieser Studie wurden ATII Zellen aus gesunden bzw. fibrotischen murinen Lungen isoliert und untersucht. Mittels Proliferations-analysen, Immunfluoreszenz, quantitativer RT-PCR sowie Microarrayanalysen, konnten wir eine gesteigerte Proliferation und veränderte Genexpression der fibrotischen ATII Zellen nachweisen. Insbesondere der WNT/β-catenin Signalweg war differenziell reguliert und aktiviert. Weitere Analysen zeigten, dass das *WNT1 inducible signalling protein* (WISP) 1 in den ATII Zellen in der experimentellen als auch humanen idiopathischen pulmonalen Fibrose vermehrt exprimiert wird. Die Stimulation von primären ATII Zellen mit rekombinanten WISP1 führte zu einer gesteigerten Proliferation und epihtelialen-mesenchymalen Transition (EMT), während eine Stimulation von humanen Fibroblasten zu einer gesteigerten Produktion und Deposition von extrazellulärer Matrix führte. In der Bleomycin-induzierten Lungenfibrose führte die Gabe von neutralisierenden Antikörpern gegen WISP1 zu einer Reduktion von profibrotischen Genen sowie EMT-Markern. Eine deutliche Abschwächung der Lungenfibrose mit verbesserter Lungenarchitektur konnte weiterhin durch immunhistochemische Analysen und Quantifizierung von Bestandteilen der extrazellulären Matrix, sowie einer Verbesserung der Lungenfunktion und des Überlebens, bestätigt werden. Unsere Studie identifiziert WISP1 als profibrotischen Mediator, der an der gestörten epithelialen-mesenchymalen Interaktion beteilgt ist. Eine Hemmung von WISP1 könnte eine mögliche neue Therapieform für Patienten mit IPF darstellen.

INTRODUCTION

Diffuse parenchymal lung diseases

Diffuse parenchymal lung diseases (DPLDs) are characterized by progressive fibrosis of the pulmonary interstitium, which subsequently leads to distortion of the normal lung architecture and respiratory failure (1). Fibrotic alterations can occur secondary to lung injury, provoked e.g. by chemotherapy, toxin inhalation, collagen vascular disease, or as an idiopathic entity in the form of idiopathic interstitial pneumonias (IIP) (1-3)}. IIPs are a heterogeneous group of rare DPLDs of unknown etiology. IIPs are divided into idiopathic pulmonary fibrosis (IPF), which is the most common form of IIP, and non-IPF. The different forms are mainly differentiated by histological, radiological and clinical features. Non-IPFs comprises of nonspecific interstitial pneumonia (NSIP), cryptogenic organizing pneumonia (COP), acute interstitial pneumonia (AIP), respiratory bronchiolitis-associated interstitial lung disease (RB-ILD), desquamantative interstitial pneumonia (DIP) and lymphocytic interstitial pneumonia (LIP). IPF differs prognostically and therapeutically from non-IPFs IIPs, which underlines the importance of a stringent diagnostic process, which includes close communication between clinician, radiologist, and pathologist (1, 2).

IPF - Clinical features

IPF exhibits a progressive course with a poor prognosis. IPF occurs mainly in people aged 50 yrs and is more common in men. The prevalence of IPF is estimated at 15-40 cases per 100000 per year, incidence 7 cases per 100000 per year. Smoking has been identified as potential risk factor. IPF has an insidious onset characterized by unexplained dyspnoea, especially on exertion, and nonproductive cough for a minimum period of 3 months (2, 4-6). Recurrent respiratory infections and an acute exacerbation are frequent and often responsible for acute deterioration (4, 7, 8). Ultimately, IPF leads to peripheral edema and right heart failure. The mean survival from the time of diagnosis is 3-5 years regardless of treatment, as IPF exhibit very limited responsiveness to currently available therapies (2, 9-11). Historically, oral corticosteroids, either

alone or in combination with immunsuppressiva have been used. Evidence for the effectiveness of these drugs from controlled studies, however, is missing (6, 12). A number of other treatments such as interferon-γ or pirfenidone have not proved effective (6, 13, 14). The antioxidant N-acetylcysteine has been shown to slow the rate of decline in lung function but does not significantly alter mortality (15). Information from these studies and consensus statements suggests that a combination of low-dose prednisolone in combination with azathioprine and antioxidant treatment is the preferred choice up to now (16). It has to be pointed out; however, that lung transplantation remains the only therapeutic intervention with a known survival benefit for IPF patients (17, 18).
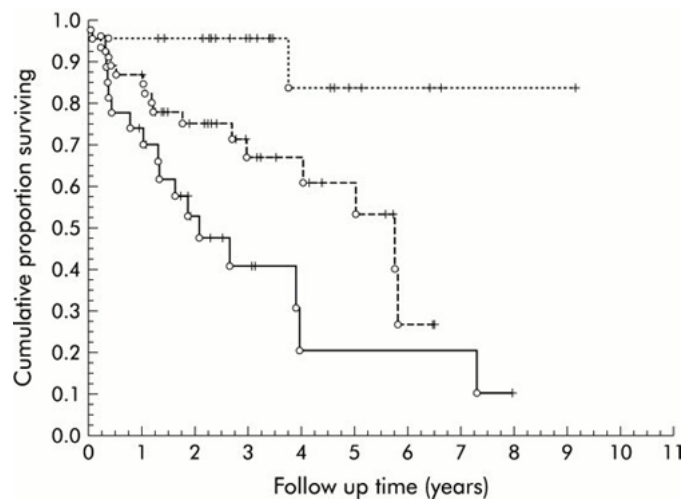

Figure I1. Kaplan-Meier survival curves for patients grouped by combining HRCT and histopathological features as follows: histopathologic pattern showing NSIP and HRCT interpreted as indeterminate or NSIP (n=23, dotted line); histopathologic pattern showing UIP and HRCT interpreted as indeterminate or NSIP (n=46, dashed line); and histopathologic pattern showing UIP and HRCT interpreted as UIP (n=27, solid line), p=0.001. + = last follow-up visit; circle = death. (19)

IPF –Pathological and histopathological features

Next to clinical features, such as age >50 yrs, dyspnoea and nonproductive cough >3 months, several major criteria are essential for the diagnosis of IPF. These include 1) the exclusion of other known causes of DPLD; 2) abnormal pulmonary function tests exhibiting restriction and impaired gas exchange; 3) bibasilar reticular abnormalities with ground-glass opacities on high resolution computer tomography, in particular lower-lobe honeycombing; and 4)

transbronchial lung biopsy or bronchoalveolar lavage, excluding other causes (1, 20-23).
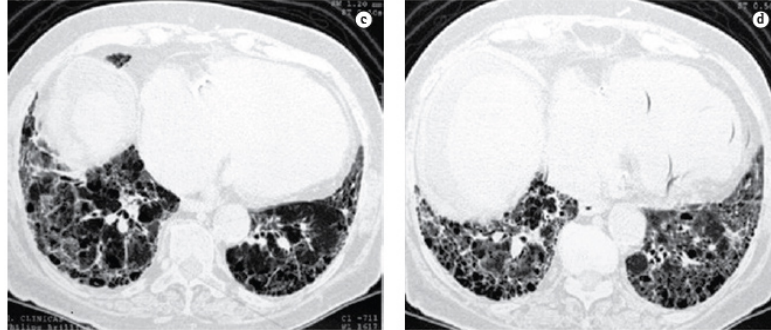

Figure I2. High-resolution computed tomography (HRCT) from an IPF patient. Peripheral reticular abnormalities with minimal ground-glass opacities and cystic structures surrounded by thickened white lines (honey combing).

A definitive diagnosis of IPF, however, requires a surgical lung biopsy and detailed histopathological analysis. The typical pathological pattern defining IPF is the usual interstitial pneumonia (UIP) pattern, which is characterized by the following observations: 1) fibrotic zones with dense collagen and scattered fibroblast foci in particular in subpleural and paraseptal areas, 2) a heterogeneous pattern with normal and abnormal lung, and 3) comparatively little nonspecific chronic inflammation compared with other IIPs (24-27). The fibroblastic foci consist of activated (myo)-fibroblasts and are a cardinal feature of UIP (26, 27). Fibroblast foci are mainly in close proximity with injured hyperplastic alveolar epithelium, largely composed of alveolar epithelial type II (ATII) cells. Interestingly, only mild inflammation is present in these areas. While historically, inflammatory processes were thought to trigger and facilitate the progression of IPF, this view has been questioned, due to the above mentioned histopathological observations and ineffectiveness of anti-inflammatory therapy in IPF (28-30). In addition, mortality of IPF patients has been correlated with the presence of fibrotic foci and adjacent failure of reepithelization, but not with inflammation (25, 31).
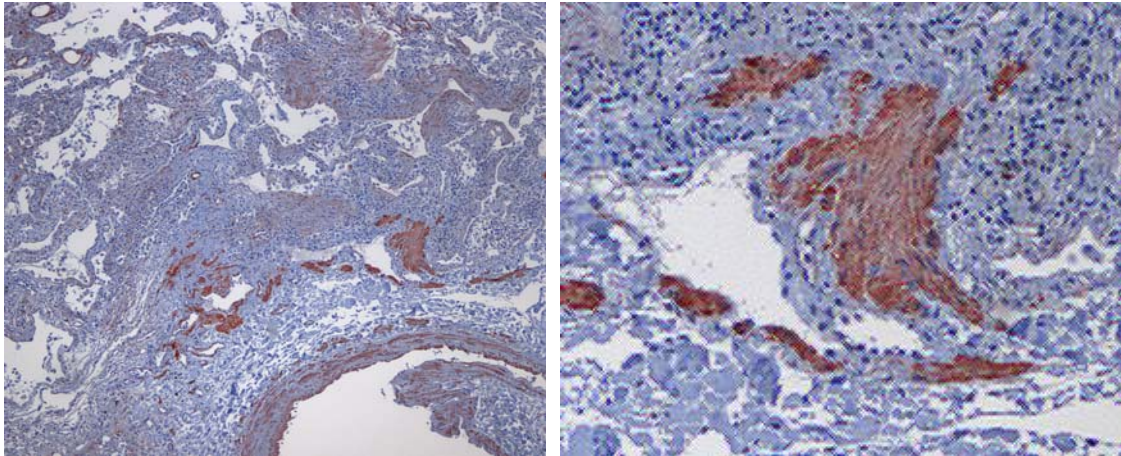
Figure I3. Histopathological pictures of IPF. Tissue sections were stained for smooth muscle actin (brown), to visualize the activated fibroblasts in fibroblast foci (magnification 10x (left) and 40x (right)).

Idiopathic pulmonary fibrosis (IPF) - Pathomechanism

Altogether, the above described observations led to the concept that repetitive alveolar epithelial injury and impaired repair mechanisms, in the presence or absence of local inflammation, play a central role in IPF/UIP pathogenesis, leading to impaired epithelial-mesenchymal interaction and fibroblast activation (28-30).

While the initial injury in IPF is affecting the alveolar epithelium, the interstitial fibroblast / activated (myo)-fibroblast represents the key effector cell responsible for the increased ECM deposition that is characteristic for IPF (32-34). Thus, a key question in IPF that needs to be elucidated is: What is the origin of the activated (myo)-fibroblast? Three major approaches exist to answer this question: First, resident pulmonary fibroblasts proliferate in response to fibrogenic cytokines and growth factors, such as transforming growth factor (TGF)-β, thereby increasing the fibroblast pool by local fibroproliferation (33, 34). Second, bone marrow-derived circulating fibrocytes cells traffic to the lung during experimental lung fibrosis, and may serve as progenitors for interstitial fibroblasts (35-37). Third, alveolar epithelial cells may turn into fibroblast-like cells, a process called epithelial-to-mesenchymal transition (EMT) (38, 39). EMT is well described in the process of embryonic development, as well as in oncogenic progression

and metastasis (40, 41). Importantly, it was recently demonstrated that TGF-β induces EMT in alveolar epithelial cells in vitro and in vivo (38, 39, 42).

The current "alveolar epithelial injury" concept of IPF/UIP further demand the following question: What are the mediators of alveolar epithelial cell injury and impaired epithelial-mesenchymal interaction in IPF? Epithelial-mesenchymal interactions are a prerequisite for proper lung development and homeostasis. In the adult lung, epithelial-mesenchymal interactions are responsible for the maintenance of the trophic alveolar unit, and are essential for normal lung function and gas exchange. Impaired epithelial-mesenchymal crosstalk between ATII cells and subepithelial fibroblasts, however, has recently been shown to contribute to the pathobiology of IPF (30, 43). Although several soluble mediators released by ATII cells, such as TGF-β1 (44), angiotensin II (45, 46), or interleukin (IL)-1β (47), have been assigned a clear pathogenic role in IPF and experimental models thereof, therapeutic options neutralizing their activity have not been successful in the clinical use as of yet (6, 48, 49). In addition, only limited information is available about the phenotype and gene regulatory networks of ATII cells in lung fibrosis.

AIM OF THE STUDY

It is well-accepted that repetitive alveolar epithelial injury and impaired repair mechanisms represents a trigger event in the development of IPF, causing impaired epithelial-mesenchymal interaction and fibroblast activation in IPF. In this study we sought to address the following key question:

"*What are the mediators of alveolar epithelial cell injury and impaired epithelial-mesenchymal interaction in IPF?*"

We aimed to

1) characterize the ATII cell phenotype in experimental and human idiopathic pulmonary fibrosis;

2) determine alterations in the gene and protein expression of ATII cells in experimental and human idiopathic pulmonary fibrosis;

3) identify new (secreted) proteins involved in epithelial-mesenchymal interactions;

4) evaluate the therapeutic suitability of identified proteins

In detail, we initially performed an unbiased whole genome microarray analysis of primary mouse ATII cells isolated from fibrotic lungs. We present a comprehensive analysis of the ATII cell phenotype in experimental and human idiopathic pulmonary fibrosis, and report altered expression of cell- and disease specific proteins in lung fibrosis *in vivo* and *in vitro*. In addition, we analyzed the effects of proteins of interest on ATII cell and fibroblast function. Moreover, we depleted the protein of interest using neutralizing antibodies in an experimental lung fibrosis model to evaluate its therapeutic potential *in vivo*.

Equipment

ABI PRISM 7500 Detection System	Applied Biosystems, USA
Bioanalyzer 2100	Agilent Technologies, USA
Developing machine X Omat 2000	Kodak, USA
Electrophoresis chambers	Bio-Rad, USA
Microscope LEICA AS MDW	Leica, Germany
Fusion A153601 Reader Packard	Bioscience, Germany
Gel blotting paper 70 × 100 mm	Bioscience, Germany
GS-800TM Calibrated Densitometer	Bio-Rad, USA
Light microscope Olympus BX51	Olympus, Germany
Microsprayer IA-1C	Penn-Century, USA
PCR-thermocycler	MJ Research, USA
Quantity One software	Bio-Rad, USA
Radiographic film X-Omat LS	Sigma-Aldrich, Germany

Reagents

Acetonitrile	Roth, Germany
Agarose	Invitrogen, UK
Albumine, bovine serum	Sigma-Aldrich, Germany
Bleomycin sulphate	Almirall Prodesfarme, Spain
CompleteTM Protease inhibitor	Roche, Germany
DAPI	Roche Diagnostics, Germany
D-(+)-Glucose	Sigma-Aldrich, Germany
D-MEM medium	Gibco BRL, Germany
D-MEM medium	Sigma-Aldrich, Germany
DNA Ladder (100 bp, 1kb)	Promega, USA
EDTA / EGTA	Promega, USA
Dulbecco's phosphate buffered saline	PAA Laboratories, Austria
ECL Plus Western Blotting Detection System	Amersham Biosciences, UK
Fetal calf serum (FCS)	Gibco BRL, Germany

Antibodies

α-smooth muscle actin (αSMA)	Chemicon International, USA
β-actin	Sigma-Aldrich, Germany
Ki67	Molecular Probes, USA
phospho-p38 MAPK (Thr180/Tyr182)	CellSignalling Technology, USA
total p38 MAPK	CellSignalling Technology, USA
phospho-p42/44 MAPK (Thr202/Tyr204)	CellSignalling Technology, USA
total p42/44 MAPK	CellSignalling Technology, USA
pro-surfactant protein C (SPC)	Chemicon International, USA
pan-cytokeratin (panCK)	Dako
tight junction protein (TJP) 1	Zymed Laboratories
α-tubulin	Santa Cruz, USA
lamin A/C	Santa Cruz, USA
CD45	BD Biosciences
CD16/32	BD Biosciences
e-cadherin (ECAD)	BD Biosciences
occludin (OCCL)	BD Biosciences
total β-catenin	CellSignalling Technology, USA
total GSK-3β	CellSignalling Technology, USA
phospho-Histone 3	CellSignalling Technology, USA
WNT1	Abcam
β-galactosidase (β-GAL)	Abcam
type 1 collagen 1 (COL1A1)	Biodesign
clara cell specific protein (CCSP)	Millipore/Upstate.
WISP1 (AF 1680, MAB 1680, MAB 1627)	R&D Systems, USA
WISP1 (ab10737)	Abcam

Recombinant proteins

WISP1, TGF-β1, WNT3A, CTGF	R&D Systems, USA

KGF was a kind gift from Veronica Grau (University of Giessen).

Mouse model of Bleomycin-induced lung fibrosis

Six to eight week-old pathogen-free female C57BL/6N mice were used throughout this study. All experiments were performed in accordance with the guidelines of the Ethic's Committee of University of Giessen School of Medicine and approved by the local authorities. Mice had free access to water and rodent laboratory chow. Bleomycin sulphate was dissolved in sterile saline solution and applied by microsprayer administered as a single dose of 0.08 mg in 200 µl saline solution per animal (≈ 5U/kg body weight). Control mice received 200 µl saline. Lung tissues were excised and snap frozen, or inflated with 4 % (m/v) paraformaldehyde in phosphate-buffered saline (PBS, PAA Laboratories) at 21 cm H_2O pressure for histological analyses.

Mouse model of WNT activation

The TOPGAL mice were purchased from Jackson Laboratories. The derivation of TOPGAL mice has been described in detail previously (50). Mice were bred under specific pathogen-free (SPF) conditions. The following primer were used for identification of transgenic animals: Lac(Z)-F 5-gttgcagtgcacggcagatacacttgctga-3´;Lac(Z)-R5´-gccactggtgtgggccataattcattcgc -3´. Four to eight week old mice were used for all experiments.

Alveolar epithelial cells isolation and culture

Primary mouse alveolar epithelial type II (ATII) cells were isolated from saline- and bleomycin-treated mice. Isolation of primary alveolar epithelial cells was performed as described by Corti *et al*. (51). Mice were killed by an overdose of isoflurane and exsanguinated by cutting the inferior vena cava. Lungs were lavaged 2× with 300 µl sterile PBS. After opening the thorax, a small incision was made in the left ventricle, a 26-gauge cannula was placed into the right ventricle and lungs were perfused with PBS until they were visually free of blood. A small cut was made into the exposed trachea to insert a shortened 21-gauge cannula that was firmly fixed and a total volume of 1.5 ml of sterile Dispase followed by 500 µl of sterile 1% low-melting agarose in PBS-/- was administered into the lungs. After 2 min of incubation, the lungs were removed and placed into a

Falcon tube containing 2ml of Dispase for 40 min. Lungs were then transferred into a culture dish containing isolation media and DNase, and the tissue was carefully dissected from the airways and large vessels. The cell suspension was sequentially filtered through 100-, 20-, and 10-µm nylon meshes and centrifuged at 200 × g for 10 min. The pellet was resuspended in isolation media and a negative selection for lymphocytes/macrophages was performed by incubation on CD16/32- and CD45-coated Petri dishes for 30 min at 37 °C. Negative selection for fibroblasts was performed by adherence for 45 min on cell culture dishes. Cell purity and viability was analyzed in freshly isolated ATII cells directly after isolation. Cell purity was routinely assessed by epithelial cell morphology and immunofluorescence analysis of panCK, pro-SPC (both positive), αSMA, and CD45 (both negative) of cytocentrifuge preparations of ATII cells. Cell viability was checked by Trypan Blue exclusion. ATII cells used throughout this study demonstrated a 95 ± 3% purity and > 97% viability. Finally, ATII cells were suspended in DMEM + 10% FCS, 2 mM L-glutamine, 100 units/ml penicillin, and 100 g/ml streptomycin, and cultured for 24h to allow attachment. Phenotypic characterisation was done after this time period. After media change cells were cultured for a maximum of 2 days in a humidified atmosphere of 5% CO_2 at 37 °C.

Primary human alveolar epithelial type II (ATII) cells were isolated as previously described (52). We isolated human ATII cells from explants after transplantation. The tissue was carefully dissected from the airways and large vessels and subsequently washed 3x in PBS -/- at 4°C. The tissue was minced manually and pipett thoroughly during enzymatic digestion with Dispase for 90min at RT. The suspension was sequentially vacuum-filtered through 100-, 50-, and 20-µm nylon meshes and centrifuged at 200 × g for 10 min. The pellet was resuspended in isolation media and a Ficoll gradient was performed. The ATII cell enriched interphase was incubated with anti- CD3 / CD14 antibodies for 30 min at 37°C followed by magnetic separation of contaminating leukocytes using the Magnetic Activated Cell Sorting (MACS) system (Miltenyi Biotec). Negative selection for fibroblasts was performed by adherence for 45 min on cell culture dishes for up

to three times. The purity and viability of ATII cell preparations was assessed as described for mouse ATII cells and was consistently >90% and >95%, respectively. Freshly isolated human ATII cells were used for gene expression analysis. The study protocol was approved by the Ethics Committee of the Justus-Liebig-University School of Medicine (AZ 31/93). Informed consent was obtained from each subject for the study protocol.

Conditioned media

Primary ATII cells were isolated and cultured in DMEM supplemented with 10% FCS. Twenty-four hours after plating, culture media and nonadherent cells were removed, attached cells washed × 2 with PBS, and cells replenished with DMEM. The cells were then cultured for another 24 h, after which conditioned medium (CM) was collected. CM was centrifuged at 2.000 g (10 min, 4°C) to remove cellular debris, and transferred to a sterile container.

Human tissues

Lung tissue biopsies were obtained from 15 IPF patients with histological usual interstitial pneumonia (UIP) pattern (4 females, 11 males; mean age = 58 ± 8 years; mean VC= 48% ± 7%; mean TLC = 50% ± 5%; mean DLCO/VA = 23% ± 3%; O2 =2–4 l/min; PaO2 = 49–71 mmHg, PaCO2= 33–65 mmHg) and 9 control subjects (organ donors; 4 females, 5 males; mean age 42 ± 10 years). Individual patient characteristics are shown in **Table S1**. Furthermore, lung tissue biopsies were obtained from four patients with NSIP pattern (mean age 55 ± 5 years; 2 females, 2 males) and six patients with chronic obstructive pulmonary disease (COPD; mean age 54 ± 4 years; 4 females, 2 males). Samples were immediately snap frozen or placed in 4% (w/v) paraformaldehyde after explantation. The study protocol was approved by the Ethics Committee of the Justus-Liebig-University School of Medicine (AZ 31/93). Informed consent was obtained in written form from each subject for the study protocol.

Laser-assisted microdissection

Laser-assisted microdissection was performed as previously described (53). In brief, 10 µm cryosections were mounted on glass slides, stained with hemalaun

for 45 s, immersed in 70% and 96% ethanol, and stored in 100% ethanol until use. Alveolar septae were selected and microdissected with a sterile 30 G needle under optical control using the Laser Microbeam System (P.A.L.M.). Microdissected tissues were then transferred into reaction tubes containing 200 µl RNA lysis buffer and samples processed for RNA analysis.

Gene expression profiling

Primary ATII cells were isolated from normal and fibrotic mouse lungs 14 days after saline or bleomycin instillation, respectively, and directly used for whole genome microarray analysis. Freshly isolated ATII cells were pooled from 6 different saline- or bleomycin-treated mice. Three independent groups of healthy and fibrotic samples were used for RNA extraction. Total RNA was extracted as described and RNA quality assessed by capillary electrophoresis using the Bioanalyzer 2100 (Agilent Technologies). All samples contained 0.3 - 1.0 µg RNA, which was preamplified and labelled using the Low Input RNA T7 kit (Agilent Technologies) according to the manufacturer's instructions. Three samples each (saline- and bleomycin-treated mice) were labelled with Cy3 and Cy5. The labelled RNA was hybridized overnight to 44K 60mer oligonucleotide spotted microarray slides (Human Whole Genome 44K; Agilent Technologies). Slides were washed with different stringencies, dried by gentle centrifugation, and scanned using the GenePix 4100A scanner (Axon Instruments). Data analysis was performed with GenePix Pro 5.0 software, and calculated fore- and background intensities for all spots were saved as GenePix results files. Stored data were evaluated using the "R" software (http://www.cran.r-project.org/) and the "limma" package from BioConductor (http://www.bioconductor.org). Experimental conditions and results from all microarray experiments are outlined in detail in the Supplement, according to the MIAME guidelines.

Reverse transcriptase (RT)-PCR and quantitative (q) RT-PCR

Total RNA was extracted using Qiagen extraction kits according to the manufacturer´s protocol, and cDNAs were generated by reverse transcription using SuperScript™ II (Invitrogen). Quantitative PCR was performed using

fluorogenic SYBR Green and the Sequence Detection System 7500 (Applied Biosystems). Hydroxymethylbilane synthase (HMBS) and hypoxanthine phosphoribosyltransferase 1 (HPRT1) for mouse and human, respectively and both ubiquitously and equally expressed genes that are free of pseudogenes, were used as reference genes in all qRT-PCR reactions. PCR was performed using the primers listed in **Table S2 and 3**, used at a final concentration of 200 nM. Relative transcript abundance of a gene is expressed in ΔCt values (ΔCt = $Ct^{reference} - Ct^{target}$). Relative changes in transcript levels compared to controls are expressed as ΔΔCt values (ΔΔCt = $ΔCt^{treated} - ΔCt^{control}$). All ΔΔCt values correspond approximately to the binary logarithm of the fold change.

Immunofluorescence/-histochemistry

For immunofluorescence analysis, cells were plated on chamber slides, fixed with acetone/methanol (1:1), and blocked for non-specific binding sites with 3% (m/vol) BSA. Fixed cells were incubated with the indicated primary antibodies for 60 min in PBS containing 0.1% (m/vol) BSA. Indirect immunofluorescence was performed by incubation with FITC-/ or Alexa 555-conjugated secondary antibodies (Zymed and Molecular Probes, respectively) for 45 min. Nuclei were visualized by 4,6-diamidino-2-phenylindole (DAPI) staining for 10 min. For immunohistochemical analysis, lungs were processed using standard procedures, embedded in paraffin, and mounted on poly-L-lysine coated slides. Antigen retrieval was performed in 6.5 mM sodium citrate, pH 6.0, in a pressure cooker, after which endogenous peroxidase activity was quenched with 3% (v/v) H_2O_2 for 20 min. Proteins of interest were visualized using the Histostain *Plus* Kit (Zymed).

Detection of β-galactosidase in TOPGAL mice

The β-galactosidase was detected using the X-GAL (5-bromo-4-chloro-3-indolyl β-D-galactosidase) reporter gene staining kit from Sigma-Aldrich. Lung tissues were excised and immediately transferred to fixative containing 0.2% glutaraldehyde, 5mM EGTA, 100mM $MgCl_2$ in 0.1 M $NaPO_4$ (pH 7.3) for 4h at 4°C with one solution change. The samples were transferred to 15% sucrose in

PBS for 4h and subsequently to 30% sucrose in PBS at 4°C overnight. Samples were embedded in Tissue-Tek O.C.T. and 15µm sections were cut. The sections were dried at RT for 2h before staining. For staining, the sections were washed twice with PBS and the X-GAL staining solution was incubated overnight at 37°C. Counterstain was performed with hemalaun.

Western blot analysis

Cells were harvested, lysed in extraction buffer [20 mM Tris-Cl, 150 mM NaCl, 1 mM EDTA, 1 mM EGTA, 1 % (v/v) Triton X-100, supplemented with Complete^{TM} Proteinase Inhibitor Cocktail (Merck Biosciences)]. Protein extracts were clarified by centrifugation (6,000 × g) at 4 °C. Protein concentrations were determined using the method of Bradford and 25 µg of total protein was separated on 10% SDS-polyacrylamide gels. Separated proteins were transferred onto nitrocellulose membranes (Invitrogen), the membranes were blocked with 5% non-fat dry milk in TBS, and incubated with the indicated primary antibodies. After washing, membranes were incubated with appropriate secondary, horseradish peroxidase-linked antibodies (Pierce). Proteins were visualized by enhanced chemiluminescence and autoradiography (ECL, Amersham Biosciences).

Proliferation assay

Primary ATII cells were plated at a density of 15×10^4/well in 48-well plates, synchronized for 24 h in serum-free medium, and treated for 24 h as indicated. Primary mouse fibroblasts or human lung fibroblasts (HFL1) cells were seeded at a density of 15×10^3/well and synchronized for 24 h in serum-free medium. ^{3}H-thymidine (0.5 µCi/ml; Amersham Biosciences, Piscataway, NJ) was added to the media for the last 6 h of each experiment. Cells were then washed 3× with PBS, lysed in 10% trichloroacetic acid, and incorporation of ^{3}H-thymidine was determined by liquid-scintillation counting. In addition, proliferation was assessed by cell counting 24 h after stimulation with WISP1, each condition counted at least three times.

Migration assay

Cell migration was determined using a Boyden chamber assay (ThinCerts™ Tissue Culture Inserts, 24 wells, pore size 3.0 µm, from Greiner Bio-One) (54). Cells were cultured for 24h to allow their attachment to the membrane, serum starved, and migration was induced by adding either WISP1 or TGF-β1 to the media in the lower wells, as indicated. After 24 h, cells were fixed and stained using crystal violet solution (Sigma-Aldrich), and non-migrated cells were removed by cotton swabbing. The number of migrated cells at the bottom of the filter was counted under a light microscope.

Collagen assay

NIH-3T3 cells or human lung fibroblasts (HFL1) were plated at a density of 30,000 cells/well in 6-well plates, synchronized for 24 h in serum-free medium, and treated for 24 h as indicated. Whole lung homogenates were used for in vivo analysis. Total collagen content was determined using the Sircol Collagen Assay kit (Biocolor). Equal amounts of protein lysates were added to 1 ml of Sircol dye reagent, followed by 30 min of mixing. After centrifugation at 10,000 × g for 10 min, the supernatant was carefully aspirated and 1 ml of alkali reagent was added. Samples and collagen standards were then read at 540 nm in a spectrophotometer (Bio-Rad). Collagen concentrations were calculated using a standard curve with acid-soluble type 1 collagen.

Small interfering RNA (siRNA) transfection

The siRNA duplexes targeting mouse *Wisp1* mRNA were obtained from Dharmacon Inc (siRNA antisense si#1: 5´-uugauugaacuuauuagccctc- 3´). The siRNAs (150 nM) were transiently transfected into primary ATII cells using Lipofectamine™ 2000 Reagent (Invitrogen) at a siRNA:Lipofectamine ratio of 1:2 (µg:µl). To control for non-specific gene inhibition of the siRNAs, a negative-control siRNA (scrambled) sequence was employed. Cells were harvested and analyzed on mRNA and protein level 24 h after the transfection.

Lung function measurement

Anaesthetized and relaxed mice were tracheotomized, placed in a small animal whole body plethysmographic chamber (Buxco), and ventilated in volume-driven mode (with a positive end-expiratory pressure (PEEP) of 0 mmHg). Before measuring lung compliance, chambers were calibrated with a rapid injection of 300 µl room air. Respiration rate was set to 20/min and ventilation pressure was recorded while inflating the lung at a tidal volume of 200 µl. Ventilator compliances are given in kPa/ml and corrected for mouse whole body weight.

Statistical analysis

All ΔCt values obtained from quantitative RT-PCR and all data derived from compliance measurements were analyzed for normal distribution using the Shapiro-Wilk test, with the assignment of a normal distribution with $p > 0.05$. Normality of data was confirmed using quantile-quantile plots. All $\Delta\Delta$Ct values were analyzed using the two-tailed, one-sample t-test. Intergroup differences of ΔCt values from patients and bleomycin-treated mice were derived using a one-tailed, two-sample t-test. Proliferation assay data were analyzed using the Wilcoxon Rank sum test and the Singed Rank test. Compliance values were analyzed using the two-tailed, two-sample t-test. All p values obtained from multiple tests were adjusted using the procedure from Benjamini & Hochberg. All results presented as mean ± s.e.m., if not otherwise stated, and were considered statistically significant when $p < 0.05$ (** $p < 0.02$, * $p < 0.05$).

RESULTS

Enhanced ATII cell proliferation in experimental lung fibrosis

We initially characterized primary ATII cells in lung fibrosis by investigating the morphology and proliferative capacity of freshly isolated ATII cells from mice subjected to bleomycin-induced lung fibrosis, as well as from time-matched, saline-treated control mice. A similar purity was observed when isolating ATII cells from control or bleomycin-treated mouse lungs [95 ± 3% of pro-surfactant protein C (SPC)-positive and α-smooth muscle actin (αSMA)-negative cells] (Figure 1).
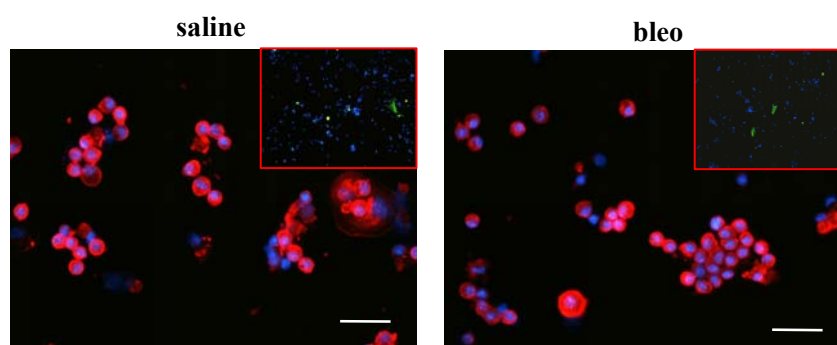
Figure 1. The purity of ATII cell isolations from saline- or bleomycin-treated mice, 14 days after instillation, as indicated, was analyzed by immunofluorescent staining. ATII cells were fixed directly after isolation (cytocentrifuge preparations) and stained with antibodies against the ATII cell marker pro-surfactant protein C (SPC; magnification: 40×, size bar = 10µm), or the (myo)-fibroblast marker αSMA (inlets, magnification: 10×).

Morphological analysis revealed the expression of the epithelial marker proteins SPC, tight junction protein (TJP) 1, e-cadherin (ECAD), as well as occludin (OCLN) (Figure 2, for secondary antibody controls see Figure S1) in both cell isolations.
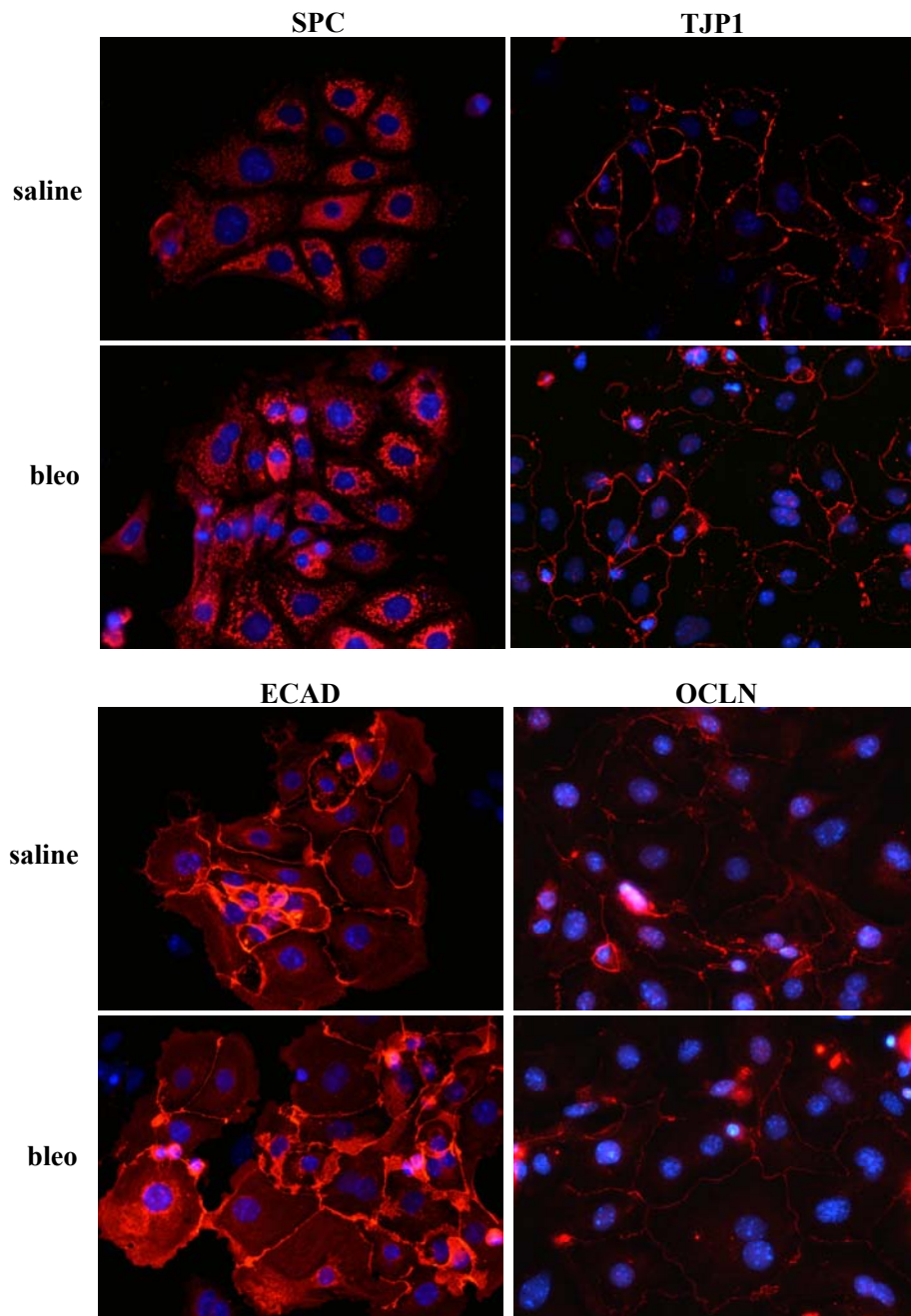
Figure 2. The phenotype of ATII cell isolations from saline- or bleomycin-treated mice, 14 days after instillation, as indicated, was analyzed by immunofluorescent staining. ATII cells were fixed after 24h of attachment and subsequently stained with antibodies against SPC, tight junction protein (TJP) 1, e-Cadherin (ECAD), or occludin (OCLN), as indicated (magnification 40×).

ATII cells isolated from the lungs of bleomycin-treated mice, however, demonstrated a significant increase in cell proliferation, as assessed by Ki67 staining and [^{3}H]-thymidine incorporation (186 - 225% of control ATII cells, 95% C.I.) (Figure 3A, B). In accordance with these observations, ATII cells from bleomycin-treated mice exhibited increased mRNA levels of the proliferation markers *Ki67*, *Cyclin G1*, and *Cyclin B2*, when compared to time-matched, saline-treated mice (Figure 4).
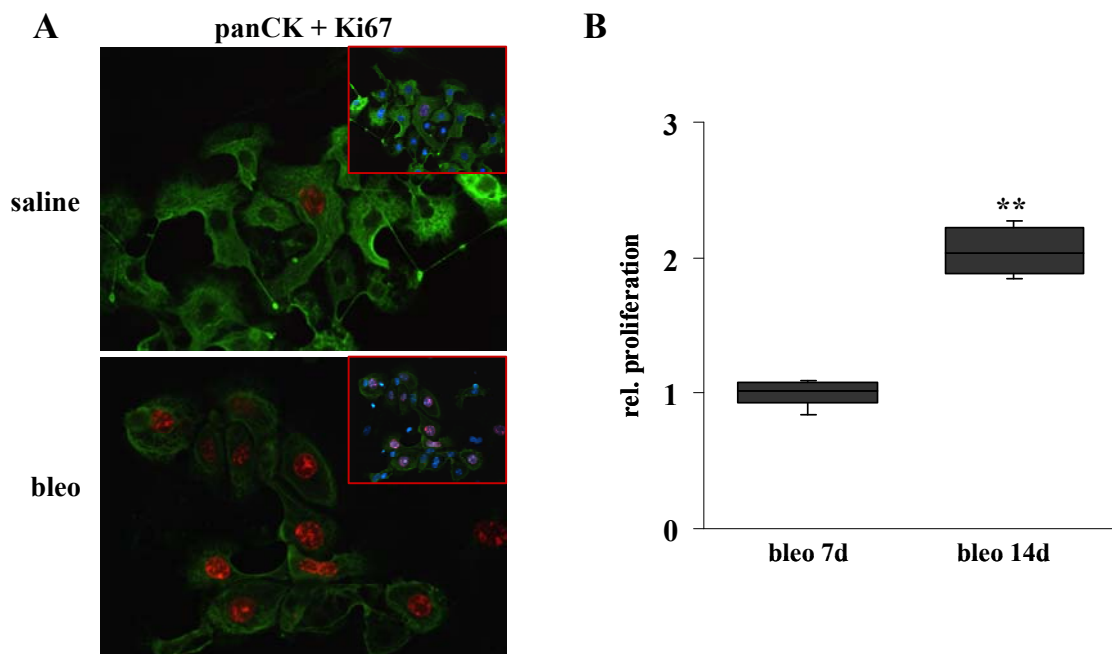
Figure 3. (**A**) Double immunostaining for panCK (green) and KI67 (red) was performed in primary ATII cells from saline- or bleomycin-treated mice, 14 days after instillation (magnification 40×). Nuclei were visualized by DAPI staining (inlet). All stainings are representative of at least three independent experiments. (**B**) ATII cell proliferation was analyzed in primary cells isolated from mice 7 or 14 d after instillation with bleomycin, as indicated, by [^{3}H]-thymidine incorporation. Data are presented as fold-change of [^{3}H]-thymidine incorporation compared with saline-instilled controls by box- and whisker plots (n = 10 per group).
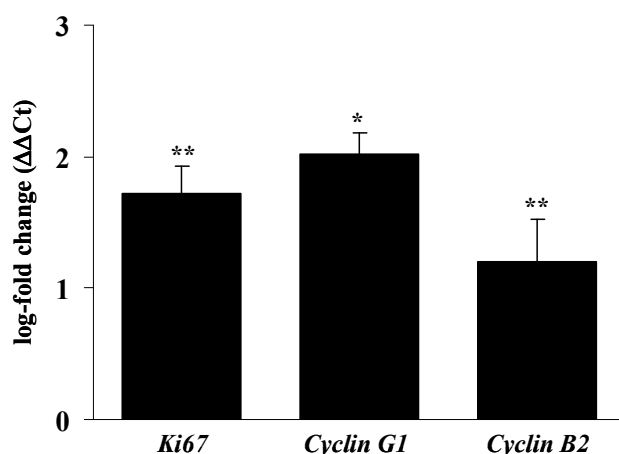
Figure 4. The mRNA levels of the proliferation markers *Ki67*, *Cyclin G1*, or *Cyclin B2* were analyzed by quantitative (q)RT-PCR using primary ATII cells and plotted as log-fold increase ($\Delta\Delta$Ct) of mRNA levels in bleomycin- *vs.* saline-treated mice, 14 days after instillation (n = 6 each). Results are presented as mean ± s.e.m., * $p<0.05$, ** $p<0.02$.

Whole genome expression profiling of ATII cells in experimental lung fibrosis

To uncover potential gene regulatory networks driving increased ATII cell proliferation, we next performed whole genome microarray analysis comparing gene signatures of freshly isolated ATII cells from bleomycin- with saline-instilled mice. As depicted in Figure 5, several gene families were differentially expressed in ATII cells obtained from fibrotic lungs. In accordance with our initial observations, ATII cells isolated from fibrotic mouse lungs demonstrated a remarkable upregulation of proliferative mediators and/or markers, such as oncogenes and cell cycle-associated genes. Furthermore, the ATII cell gene expression profile also indicated an enrichment of inflammatory stimuli and pro-inflammatory cytokines in experimental lung fibrosis, suggesting that, at least in the mouse, this is part of the alveolar epithelial cell response to fibrogenic stimuli.
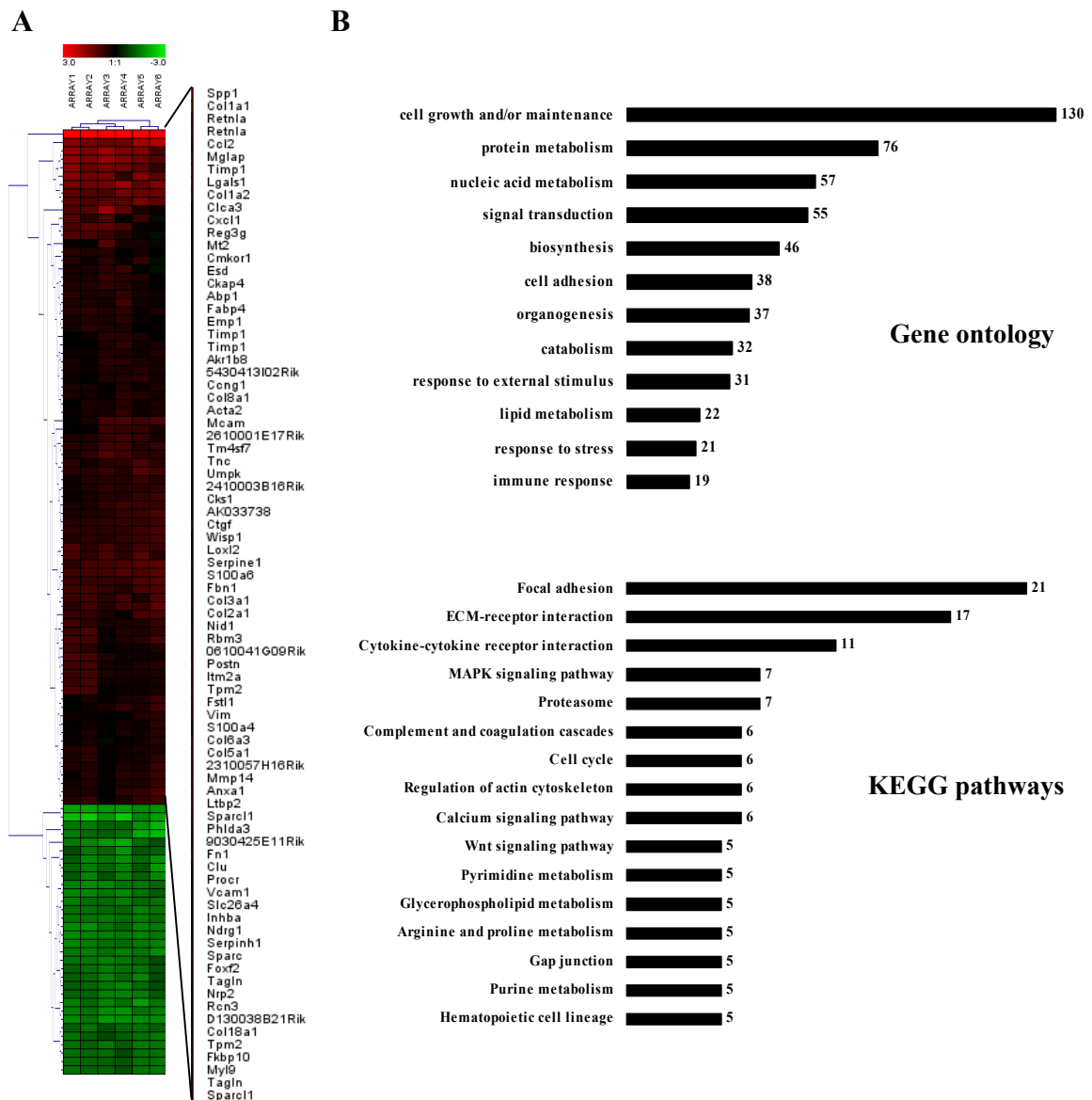
Figure 5. (**A**) ATII cell gene expression profiles were analyzed by whole genome expression analysis using RNA from freshly isolated ATII cells from saline- or bleomycin-treated mouse lungs 14 d after administration. Red and green indicate increased and decreased gene expression levels, respectively, in ATII cells isolated from bleomycin- vs. saline-treated mice. Columns represent individual samples, including dye-swap experiments. Selected genes are represented in rows. (B) Functional annotation of regulated gene clusters was performed according to Gene Ontology (GO) or the Kyoto Encyclopedia of Genes and Genomes (KEGG), as indicated.

Differentially expressed transcripts also included genes that have previously been reported to be upregulated in bleomycin-induced lung fibrosis and IPF, including *Spp1* (55, 56), *Timp1* (57), *Sfrp1*(58), and *Pai1* (59).

To confirm these findings, the gene expression profiles were further investigated in an independent set of freshly isolated, and short term cultured (48h) ATII cells by quantitative (q)RT-PCR (Figure 6), essentially giving consistent gene regulatory findings.
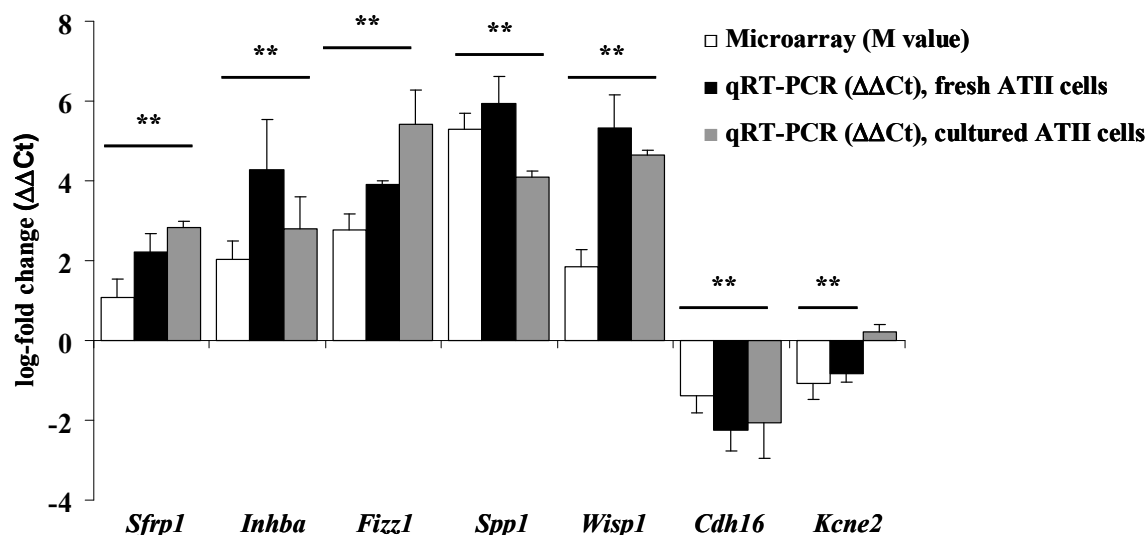

Figure 6. Confirmation of microarray results was performed for selected genes in freshly isolated ATII cells (n = 6), as well as in ATII cells 72 h after isolation (n = 3) by qRT-PCR, as indicated. Following genes were analyzed: secreted frizzled-related protein (*Sfrp*) 1, inhibin beta A (*Inhba*), found in inflammatory zone (*Fizz*) 1, secreted phosphoprotein (*Spp*) 1, WNT1-inducible signalling pathway protein (*Wisp*) 1, cadherin (*Cdh*) 16, and potassium voltage-gated channel subfamily E member (*Kcne*) 2. Results are presented as mean ± s.e.m., **p<0.02 for all bars, compared with ATII cells isolated from saline-treated mice.

Of interest, the expression of genes of the WNT signalling pathway (*Wnt10a*, *Sfrp1*, *Tcf4*, *Cyclin D1*) was upregulated in ATII cells during bleomycin-induced lung fibrosis. In particular, expression of the WNT1 inducible signalling protein (*Wisp*) 1, a member of the recently described CCN family of secreted signalling molecules (60, 61), was highly upregulated.

The WNT family of highly conserved secreted growth factors is essential to organ development and known to determine epithelial cell fate (62, 63). The canonical WNT signalling pathway, or β-catenin-dependent pathway, regulates gene transcription by stabilization of β-catenin. Upon WNT stimulation, receptor activation leads to glycogen synthase kinase (GSK)-3β phosphorylation, thereby

preventing β-catenin phosphorylation by GSK-3β. As a result, β-catenin accumulates, translocates to the nucleus, and regulates target gene expression via interaction with the T-cell-specific transcription factors (TCF) (62, 63) (Figure 7).
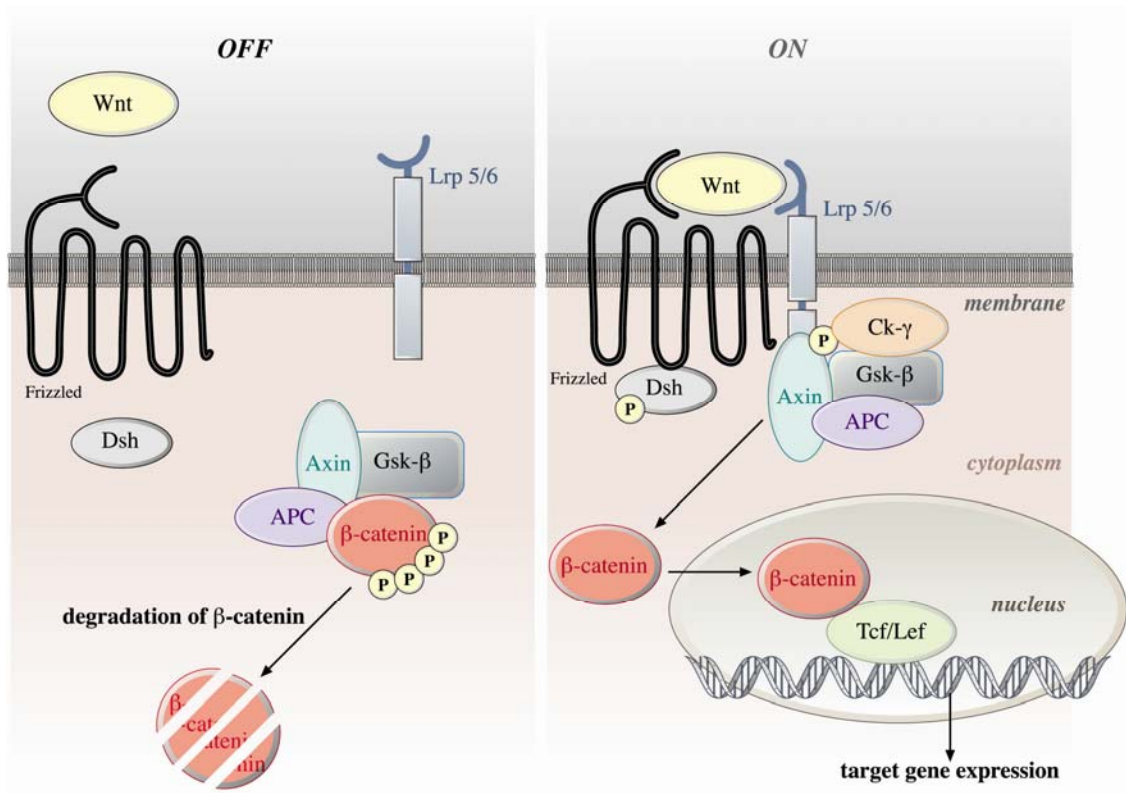

Figure 7. Canonical WNT signalling scheme.

Increased expression of WNT/β-catenin signalling molecules in lung epithelial cells during experimental lung fibrosis

To further elucidate, whether WNT/β-catenin activation is an early event in experimental lung fibrosis, as indicated by our initial gene expression analysis, we sought to quantify the mRNA expression of canonical WNT/β-catenin signalling components in ATII cells isolated from the lungs of bleomycin or saline-treated mice. The investigated WNT ligands were variably expressed in ATII

cells, and *Wnt1*, *Wnt2*, *Wnt7b* and *Wnt10b* mRNA levels were markedly upregulated, whereas *Wnt3a* was significantly downregulated (Figure 8). The common WNT receptors frizzled (*Fzd*), as well as the intracellular signal transducers *Gsk-3β*, *β-catenin*, and *Tcf4* were expressed in ATII cells, with a relative high abundance of β-catenin. *Fzd1* and *Gsk-3β* were significantly upregulated in ATII cells of bleomycin-treated mice (Figure 9).
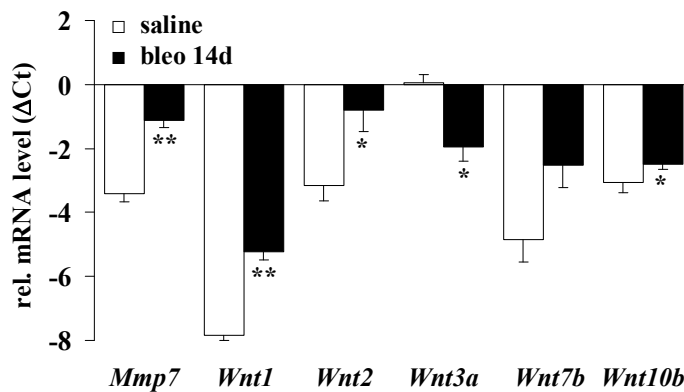

Figure 8. The mRNA levels of the WNT target gene *Mmp7*, the WNT ligands *Wnt1*, *Wnt2*, *Wnt3a*, *Wnt7b*, and *Wnt10b* were assessed in ATII cells isolated from bleomycin- and saline-treated mice (n = 6 each) by qRT-PCR. Results are presented as mean ± s.e.m., * p<0.05, ** p<0.02, as indicated.
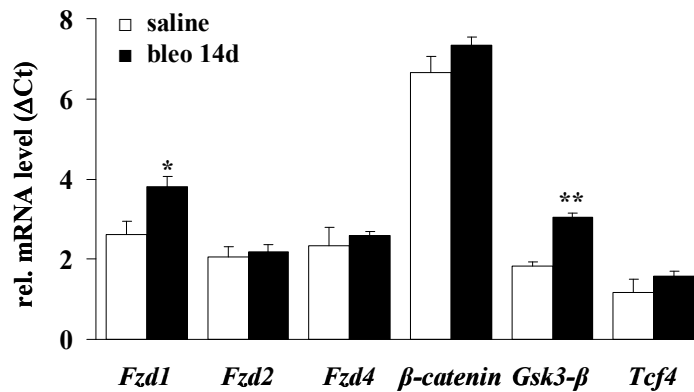

Figure 9. The mRNA levels of the receptors frizzled (Fzd) 1, 2, 4, and the intracellular signal transducers Gsk-3β, β-catenin, and Tcf4 were assessed in ATII cells isolated from bleomycin- and saline-treated mice (n = 6 each) by qRT-PCR. Results are presented as mean ± s.e.m., * p<0.05, ** p<0.02, as indicated.

Active WNT/β-catenin signalling in vivo during the development of experimental lung fibrosis

TOPGAL reporter mice were used next to localize the activation of the WNT/β-catenin pathway *in vivo* in experimental lung fibrosis. The detailed treatment scheme is outlined in Figure 10.
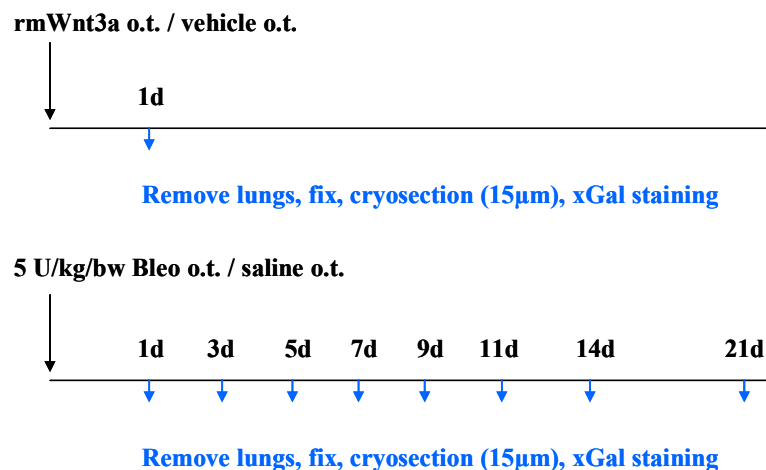
rmWnt3a o.t. / vehicle o.t.

1d

Remove lungs, fix, cryosection (15µm), xGal staining

5 U/kg/bw Bleo o.t. / saline o.t.

1d 3d 5d 7d 9d 11d 14d 21d

Remove lungs, fix, cryosection (15µm), xGal staining

Figure 10. Treatment scheme of TOPGAL mice. Recombinant mouse WNT3A or vehicle control was administered orotracheally (500 ng or 1000 ng in 80µl total volume) and mouse lungs were excised after 24h for the detection of β-galactosidase in the challenged TOPGAL mice. In a second arm, TOPGAL reporter mice were challenged with Bleomycin or saline as described in detail in Material & Methods and analyzed on different time points, as indicated. At least four mice per time point were analyzed.

Mice were treated orotracheally with either recombinant WNT3A to demonstrate the capability of the lung to activate WNT/β-catenin signalling (Figure 11, upper panel), or bleomycin to induce lung fibrosis (Figure 11, lower panel). As depicted, bronchial and alveolar epithelial cells routinely stained for β-galactosidase (β-GAL), in response to WNT3A or bleomycin. Examination of mouse lungs harvested at different time points after a single administration of bleomycin revealed an activation of WNT/β-catenin signalling as early as 5 days after the initial injury, with distinct bronchial and alveolar epithelial cells responding to WNT activation (Figure 11).
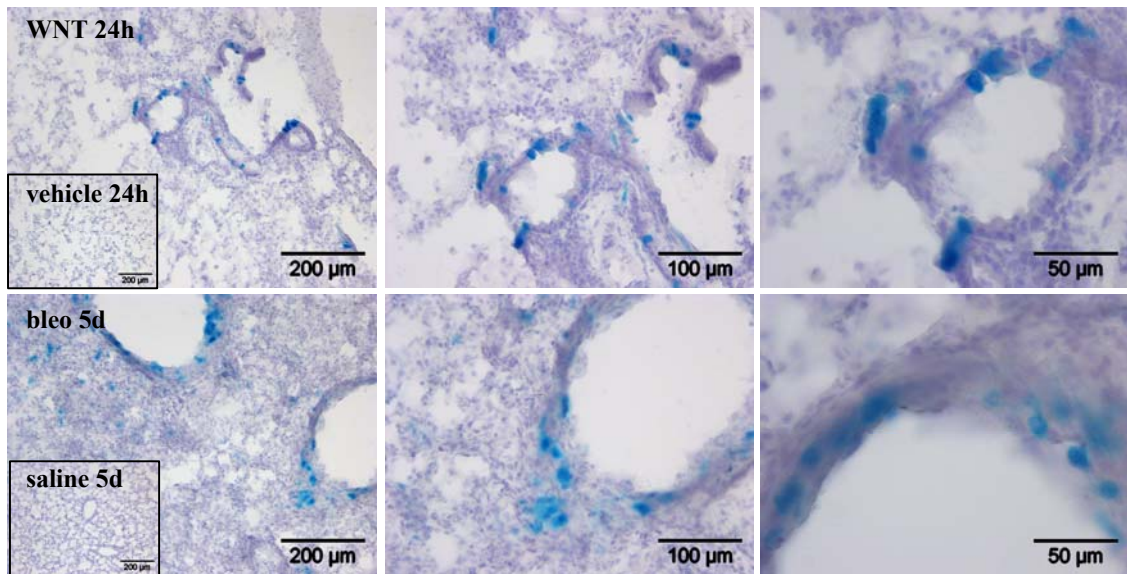
Figure 11. TOPGAL reporter mouse were treated orotracheally with WNT3A or bleomycin, as described in detail in Material & Methods. The X-GAL staining of β-galactosidase activity in lungs from WNT3A- and vehicle- treated mice (A, upper panel), or bleomycin- and saline-treated mice (A, lower panel) were performed. Pictures are representative of at least two independent experiments using at least four different lung tissues for each condition, the magnifications are indicated by scale bars.

The epithelial nature of cells with active WNT signalling was further confirmed by colocalization of β-GAL and the ATII cell marker SPC, or the clara cell specific protein (CCSP), respectively (Figure 12).
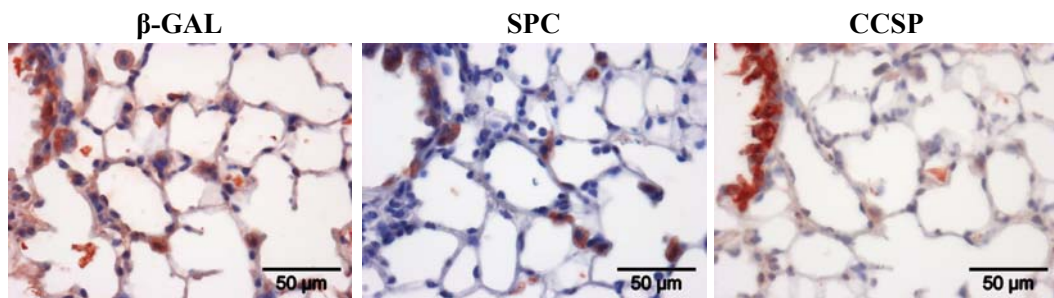

Figure 12. β-GAL, SPC, and clara cell specific protein (CCSP) protein expression in serial whole lung sections from bleomycin-treated TOPGAL reporter mouse was assessed by immunohistochemistry, the magnification is are indicated by the scale bar.

Increased expression of the WNT target genes *Cyclin D1* and *Wisp1* upon WNT3A stimulation in primary ATII cells in vitro further confirmed these results (Figure 13).
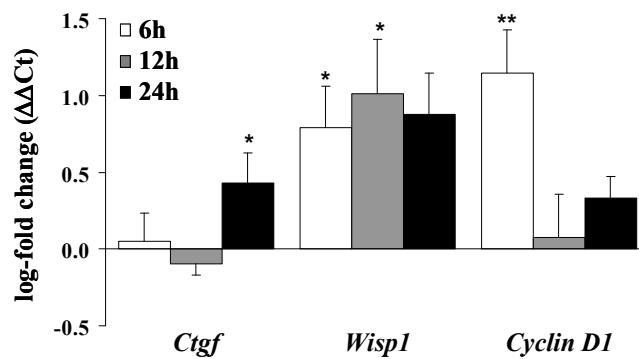

Figure 13. Primary ATII cells were stimulated with WNT3A (100 ng/ml) and the mRNA levels of *Ctgf*, *Wisp1*, and *Cyclin D1* were analyzed by qRT-PCR (n = 4 for each) at the indicated time points and plotted as log-fold increase ($\Delta\Delta$Ct) of mRNA levels in WNT-stimulated vs. unstimulated cells. Results are presented as mean ± s.e.m., * $p<0.05$, ** $p<0.02$.

Increased expression of WISP1 in ATII cells in vitro and in vivo in experimental pulmonary fibrosis

Based on the evidences, that 1) the WNT target WISP1 was one of the most regulated genes in ATII cells isolated from fibrotic mouse lungs, and 2), active WNT signalling is present in lung fibrosis, we continued our further studies on WISP1 as a potential novel mediator and amenable therapeutic target. WISP1 is a member of the CCN family of matricellular proteins, which consist of CYR61/CCN1, CTGF/CCN2, NOV/CCN3, WISP1/CCN4, WISP2/CCN5, WISP3/CCN6 (60, 64, 65). CCN proteins are comprised of four conserved cysteine-rich modular proteins. They act trough binding to specific integrin receptors and heparin sulfate proteoglycans, or modulate the activities of other growth factors and cytokines, thereby triggering a variety of cell functions, such as mitosis, adhesion, and migration of multiple cell types (64) (Figure 14). CCN family members were associated with different developmental and disease processes, however, little is known about WISP1 and WISP2.
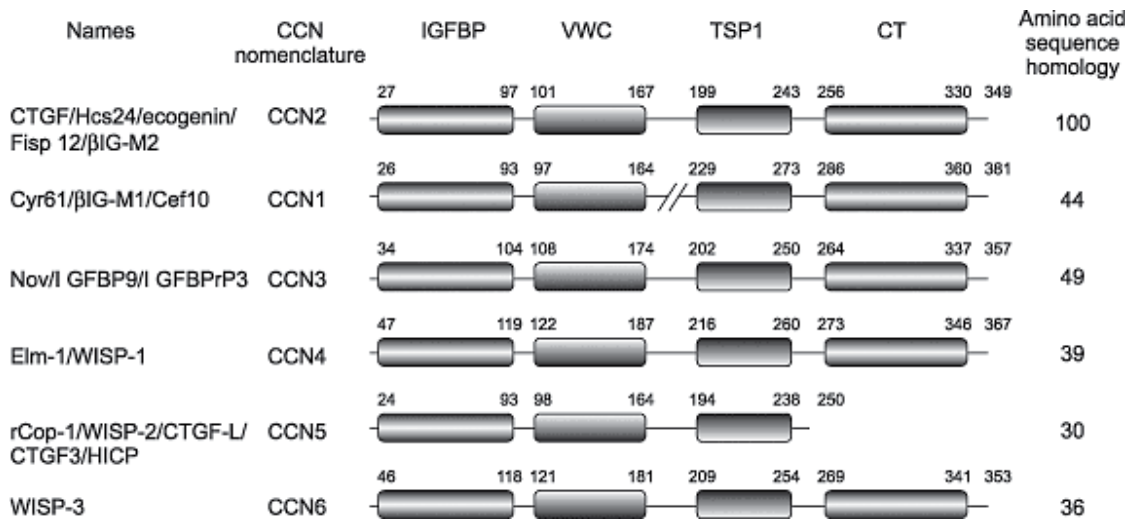
Figure 14. The CCN protein family (66).

We next analyzed the expression of all CCN family members *in vivo* in mice subjected to bleomycin-induced lung fibrosis. Of all six CCN family members, *Wisp1* mRNA exhibited the highest fold-induction in lung homogenates during bleomycin-induced lung fibrosis (Figure 15).
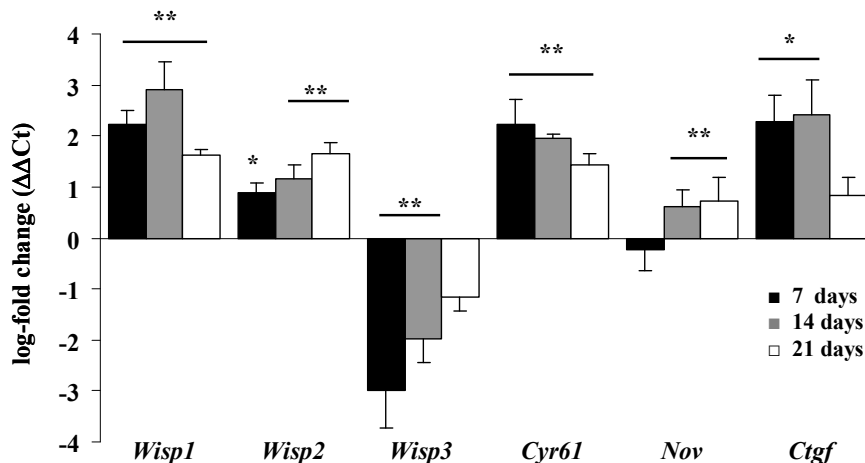

Figure 15. A time-course for CCN family member gene expression was performed using qRT-PCR of lung homogenates harvested 7, 14, or 21 d after administration of bleomycin. Respective mRNA levels were plotted as log-fold change (ΔΔCt) of mRNA levels in bleomycin- vs. time-matched saline-treated mice (n = 4), and presented as mean ± s.e.m., * p<0.05, ** p<0.02.

Furthermore, WISP1 protein localized to ATII cells *in vivo* as documented by immunohistochemistry and increased expression thereof in lung homogenates was demonstrated by Western blot analysis (Figure 16).
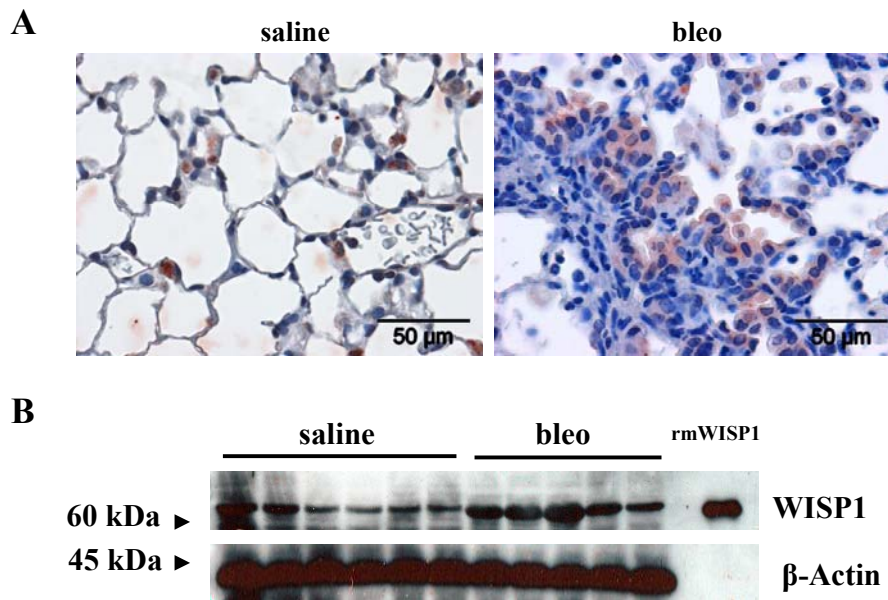

Figure 16. (A) WISP1 protein expression was assessed using immunohistochemical staining of whole lung sections of bleomycin- or saline-treated mice 14 d after application (upper panel, magnification as indicated) and **(B)** Western blot analysis in total protein lysates (lower panel). Recombinant mouse WISP1 protein served as a positive control, β-Actin served as a loading control. Data are representative of at least two independent experiments using six (saline) or five (bleo) different lung tissues each.

In support, *Wisp1* mRNA exhibit the highest fold-regulation of all CCN family members in isolated ATII cells, but not primary fibroblasts, isolated from bleomycin-treated mouse lungs (Figure 17), underlining that WISP1 originates from ATII cells during lung fibrosis. WISP1 expression was increased at the protein level in isolated ATII cells, as documented by co-immunofluorescence staining of WISP1 and ECAD (Figure 18).
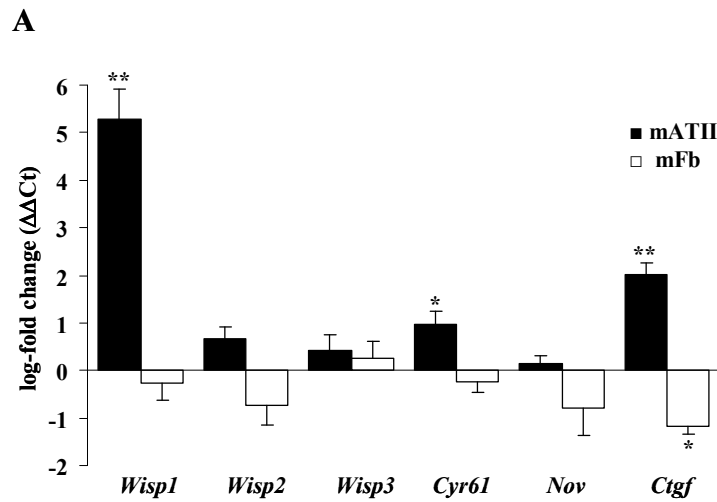
A

Figure 17. The mRNA levels of all CCN family members were determined by qRT-PCR in primary ATII cells (black bars, n = 6) or primary fibroblasts (open bars, n = 4) isolated from the lungs of saline- or bleomycin-treated mice 14 d after administration. Results are plotted as log-fold change (ΔΔCt) of mRNA levels in bleomycin-derived vs. saline-derived cells, and presented as mean ± s.e.m., * p<0.05, ** p<0.02.
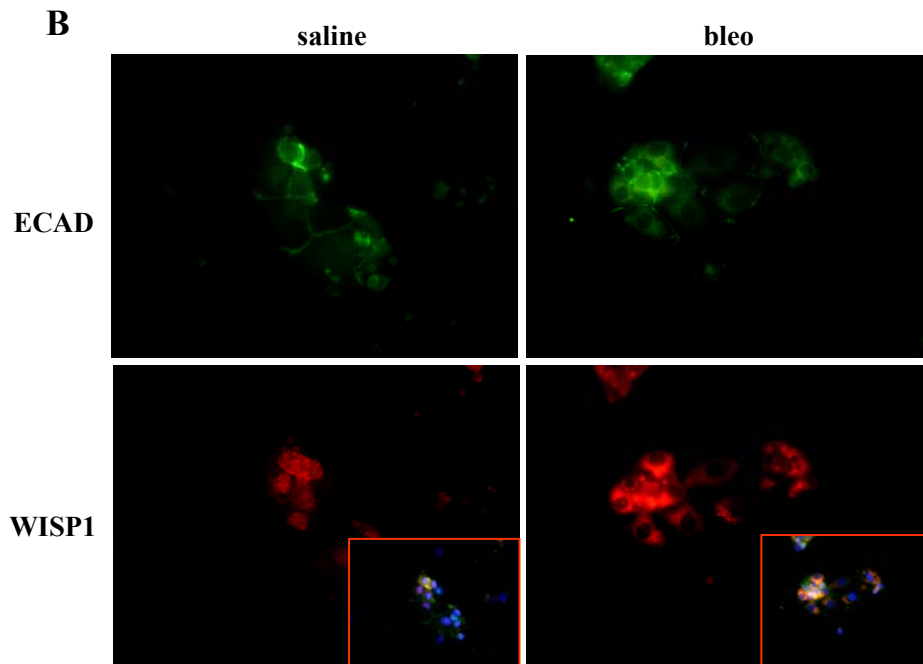
B

Figure 18. WISP1 protein expression was assessed using double immunostaining for ECAD (green) and WISP1 (red) of primary ATII cells from saline- or bleomycin-treated mice, respectively (magnification 40×). Nuclei were visualized by DAPI staining (inlet). Data are representative for at least three independent experiments.

Increased expression of WISP1 in ATII cells in vitro and in vivo in idiopathic pulmonary fibrosis (IPF)

We next sought to investigate whether increased WISP1 expression was also evident in human lung tissues derived from IPF patients. To this extent, we analyzed the mRNA levels of all CCN family members in lung specimen obtained from IPF (UIP pattern) or control (transplant donors) patients. With the exception of *WISP3*, all CCN family members were expressed in human lungs (Figure 19). *WISP1* demonstrated the lowest overall lung mRNA expression, but the highest relative differences comparing IPF with donor lung homogenates.
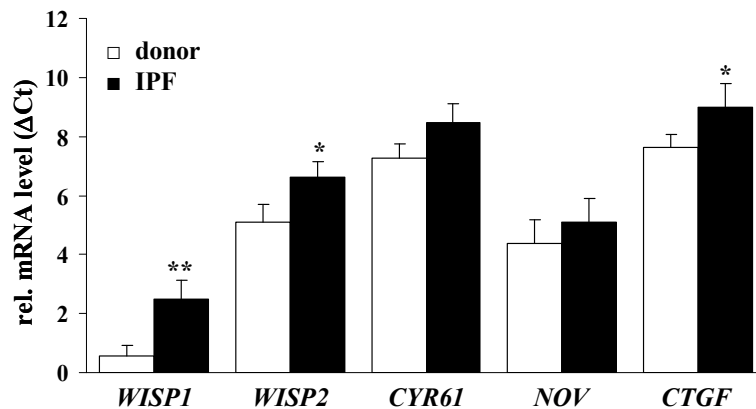
Figure 19. The mRNA levels of the CCN family members were analyzed by qRT-PCR using lung homogenates derived from donor or IPF lung explants (n = 10 each), as indicated.

Furthermore, increased expression of *WISP1* mRNA was detectable in laser-assisted microdissected septae obtained from IPF and donor lungs (Figure 20A). The qRT-PCR analysis of primary human ATII cells and fibroblasts further revealed that *WISP1*, and to a lesser extent connective tissue growth factor (*CTGF*), was highly upregulated in ATII cells, but not in primary fibroblasts obtained from IPF patients (Figure 20B).

A

B

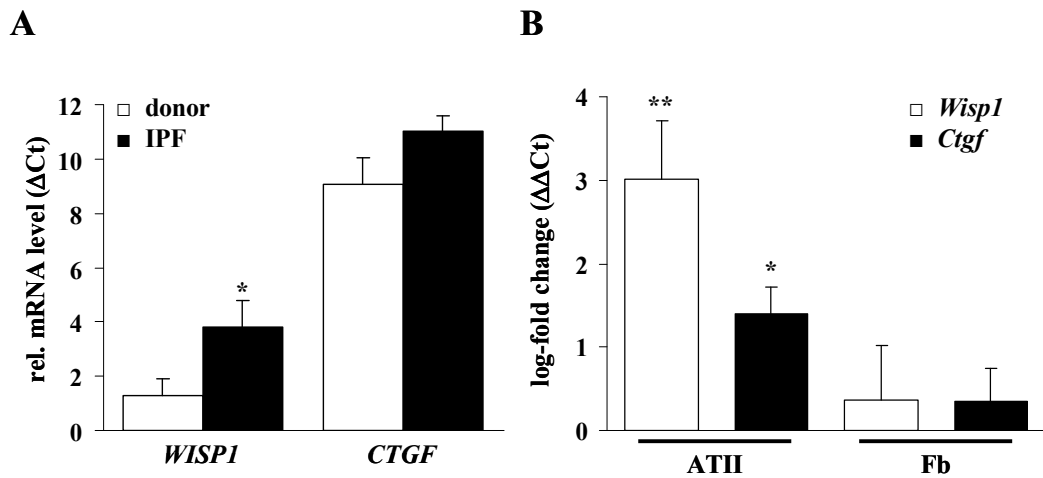**Figure 20. (A)** The mRNA levels of *Wisp1* and *Ctgf* were analyzed by qRT-PCR in microdissected septae from donor or IPF lungs (n = 5 each). Results are plotted as relative mRNA levels (ΔCt) and presented as mean ± s.e.m., * p<0.05, ** p<0.02. **(B)** The mRNA levels of *Wisp1* (open bars) and *Ctgf* (black bars) were determined by qRT-PCR in primary human ATII cells (n = 4) or fibroblasts (n = 3) isolated from donor or IPF lung tissue, as indicated. Results are plotted as log-fold increase ($\Delta\Delta$Ct) of mRNA levels in IPF-derived vs. donor-derived cells and presented as mean ± s.e.m., * p<0.05

Consistently, WISP1 localized to hyperplastic, proliferating ATII cells in close proximity to epithelial lesions and fibroblast foci in IPF (Figure 21, for antibody control see Figure S2), as assessed by staining of WISP1 and phospho-histone H3 in serial sections. WISP1 protein expression was increased in tissue samples from IPF patients, as determined by Western Blot analysis (Figure 22A). Importantly, increased expression of WISP1 was specific for IPF, whereas in other lung disorders, such as non specific interstitial pneumonia (NSIP) or chronic obstructive pulmonary disease (COPD), no regulation of *WISP1* mRNA was observed (Figure 22B).
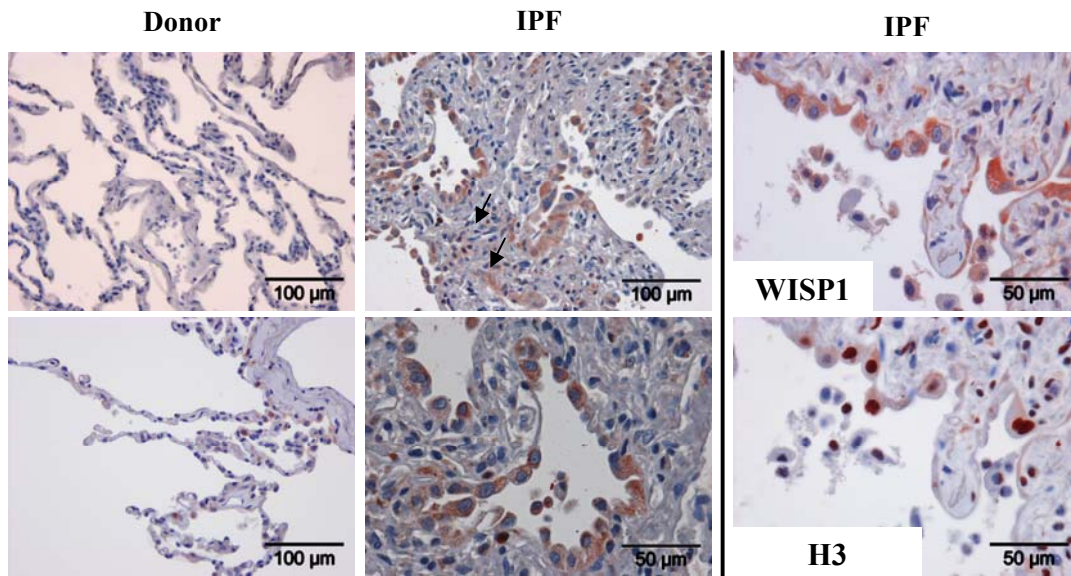
Figure 21. WISP1 protein expression in sections from control or IPF lung specimen was assessed by immunohistochemistry, the magnification is indicated by the scale bars. Arrows point to extracellular WISP1 staining. WISP1 and Phospho-Histone 3 (H3) protein expression in serial whole lung sections from IPF patients (right panel). Data are representative of at least two independent experiments using at least four different lung tissues from IPF specimens.
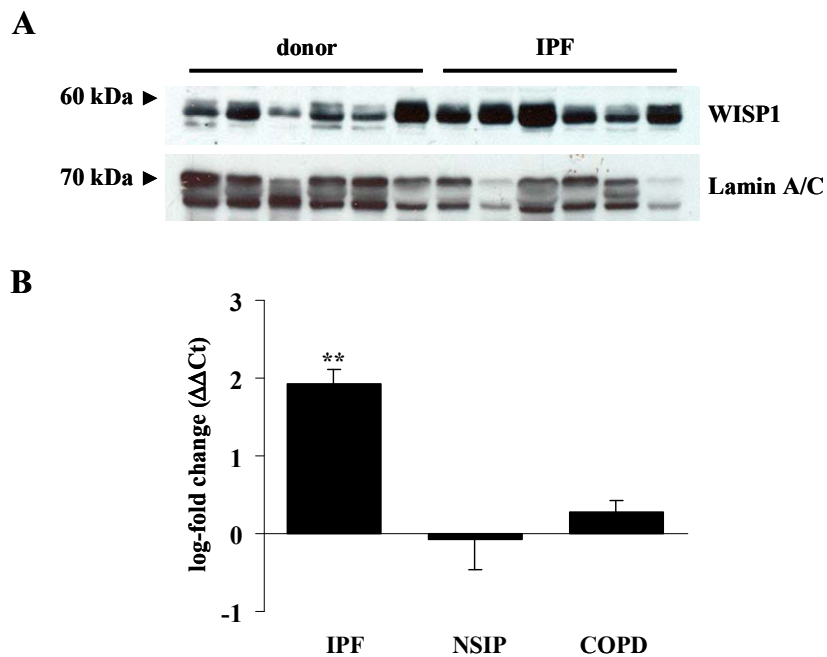
Figure 22. (**A**) WISP1 protein expression was determined in total protein lysates from donor or IPF lung tissue by Western blotting. Lamin A/C was used as a loading control. Data are representative of at least two independent experiments using six different lung tissues for donors and IPF. (**B**) The mRNA levels of *Wisp1* were analyzed by qRT-PCR using lung homogenates derived from IPF (n = 6), NSIP (n = 4) or COPD (n = 6) lung explants, as indicated. Results are plotted as log-fold increase ($\Delta\Delta$Ct), compared with control lungs (transplant donor), and presented as mean ± s.e.m., * p<0.05, ** p<0.02.

Increased ATII cell proliferation and profibrotic marker release in response to WISP1

To begin to delineate the functional contribution of WISP1, the effect of recombinant WISP1 on ATII cells was assessed next. WISP1 treatment exerted a strong proliferative effect on primary ATII cells (Figure 23 and 24, 154 - 220%, 95% C.I.), which was more pronounced than that of CTGF or keratinocyte growth factor (KGF) (Figure 24A). In contrast, ATII cells obtained from bleomycin-treated animals were not responsive to WISP1 stimulation (bleo: 186 - 213% vs. bleo + WISP1: 199 - 215%) (Figure 24A).
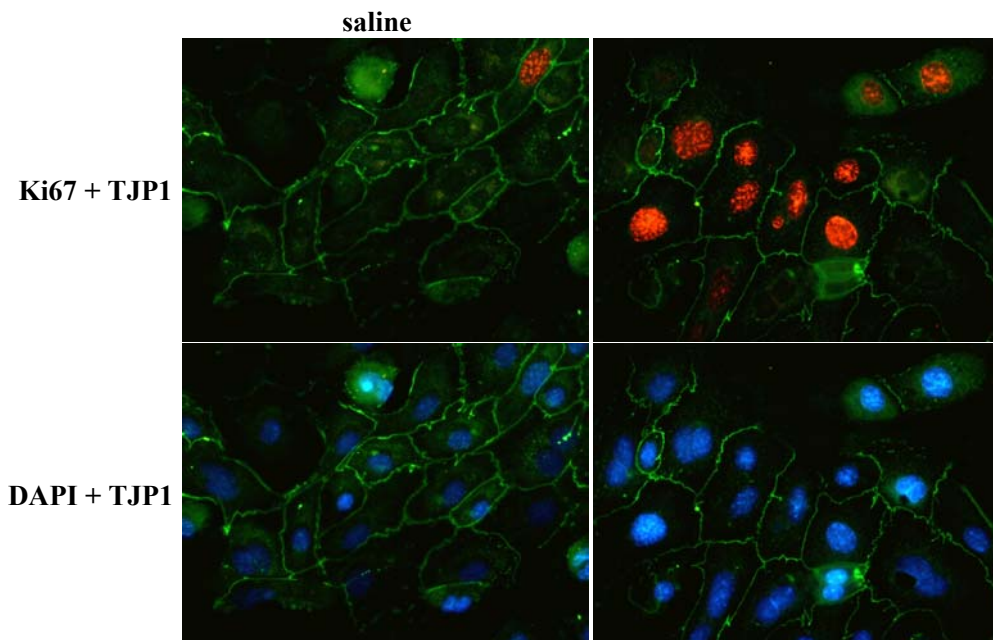
Figure 23. The effect of WISP1 (1 µg/ml, 24 hrs) on the proliferation of primary ATII cells was assessed by co-immunostaining of Ki67 (red) and TJP1 (green) (magnification 40×). Nuclei were visualized by DAPI staining (blue).

Since these cells secreted higher amounts of WISP1 (Figure 16-18), thereby driving a proliferative response, we sought to neutralize WISP1 using two different approaches: As depicted in Figure 24B, WISP1 antagonism using neutralizing antibodies attenuated the increased baseline proliferation of fibrotic ATII cells (bleo + αWISP1: 103 - 148%).
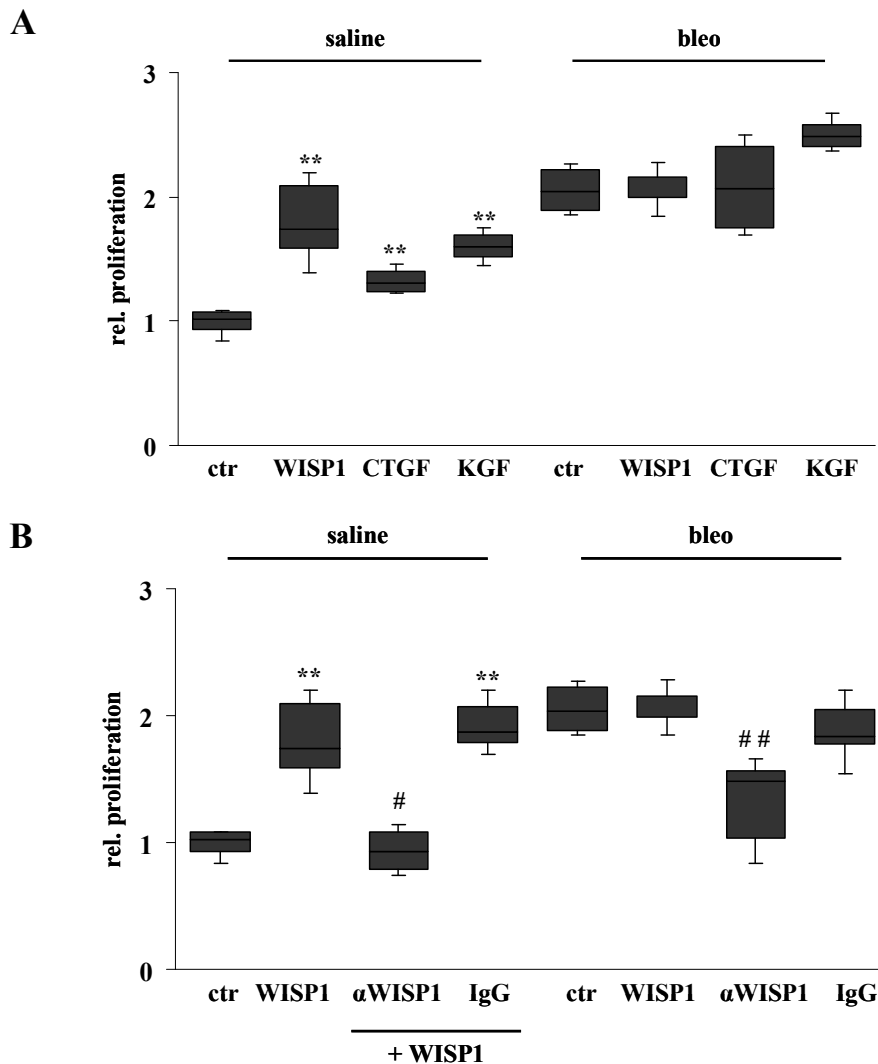
Figure 24. (**A**) The effects of WISP1 (1 µg/ml), CTGF (2.5 ng/ml), or KGF (10 ng/ml) on primary mouse ATII cell proliferation were assessed by [^{3}H]-thymidine. (**B**) The effects of neutralizing αWISP1 antibodies (20 µg/ml αWISP1) or pre-immune serum (IgG control), each applied 30 min prior to the addition of WISP1, was analyzed. Data are presented as relative proliferation, compared with unstimulated ATII cells isolated from saline-treated mice (n = 10 upper panel, n = 5 lower panel), ** p<0.02 vs. control, # p<0.02 vs. WISP1 stimulation, ## p<0.02 vs. control bleo.

Second, these results were confirmed using small interfering (si)RNA against *Wisp1* (Figure 25). The mRNA and protein knockdown efficiency is depicted in Figure 25 A and B. The knockdown of *Wisp1* led to decreased proliferation of primary ATII cells isolated from bleomycin- and saline-treated mouse lungs, as analyzed by cell counting (Figure 25C) and [^{3}H]-thymidine incorporation (Figure 25D), respectively.
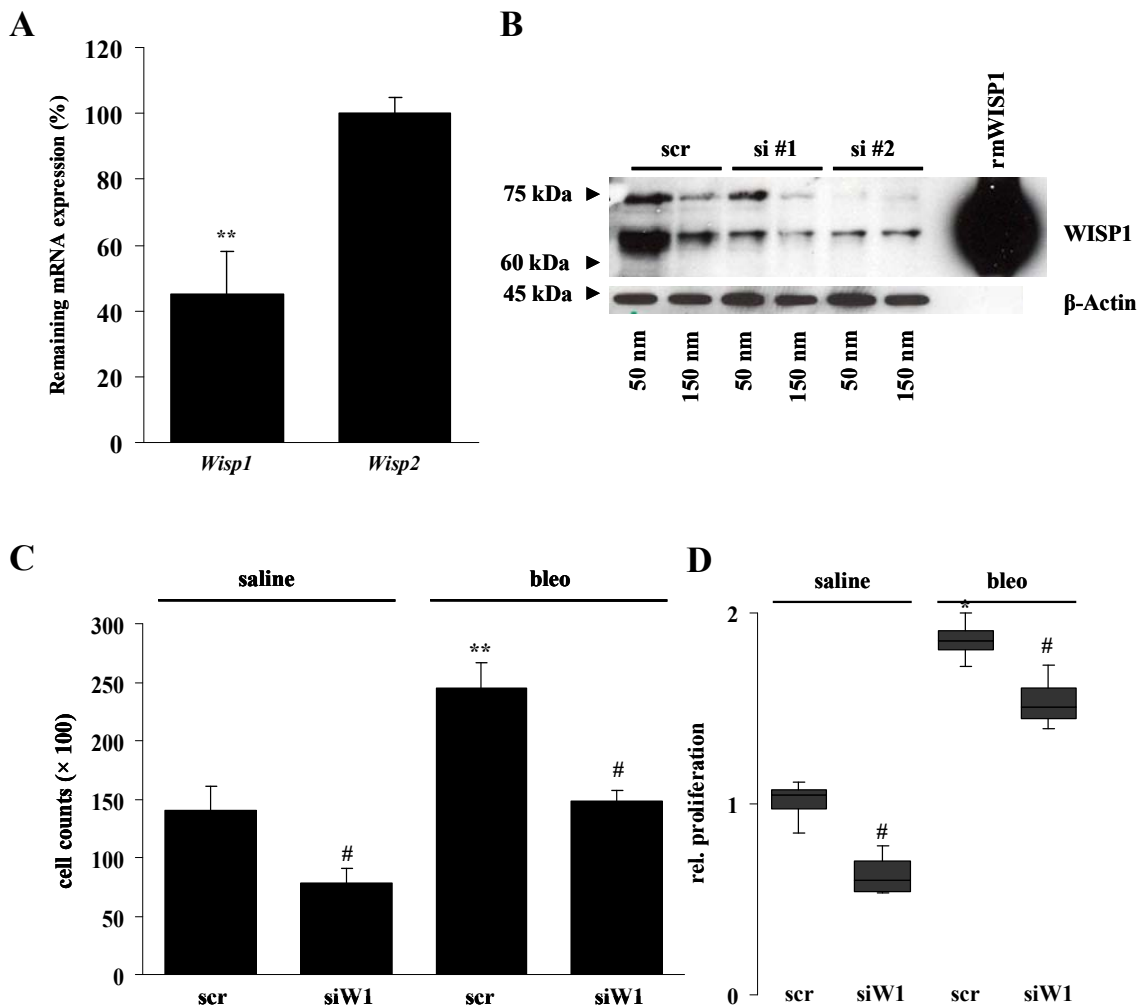
Figure 25. The Wisp1 knockdown was analyzed by qRT-PCR (A) and Western Blot (B). Two different siRNA sequences were tested in different concentrations, as indicated. Cells were harvested and lysed 24 h after transfection. For all further experiments si #1 (150 nm) was used., (C, D) Proliferation of ATII cells subjected to scrambled (scr) or *Wisp1* siRNA (siW1) treatment (150 nM each) was assessed by cell counting 24 h after treatment (C)or ^{3}H-thymidine incorporation (D). ** $p < 0.02$ bleo vs. saline, # $p < 0.02$ siRNA vs. scrambled.

Epithelial-to-mesenchymal transition (EMT) in response to WISP1

EMT is the reversible phenotypic switching of epithelial to fibroblast-like cells, and has recently gained recognition as a possible mechanism that increases the (myo)-fibroblast pool in pulmonary fibrosis (67, 68). It has been demonstrated that TGF-β represents a main inducer and regulator of EMT in multiple organ systems (38, 39), but little is known about other cytokines or mediators that are able to induce EMT during lung fibrosis. Here, we show that WISP1 treatment of primary ATII cells led to decreased mRNA levels of *Tjp1*, *eCad* and *Occl*, but

elevated mRNA levels of *Fsp1* and *αSMA*, as analyzed by qRT-PCR, indicating that WISP1 is a potent inducer of EMT in ATII cells *in vitro* (Figure 26).
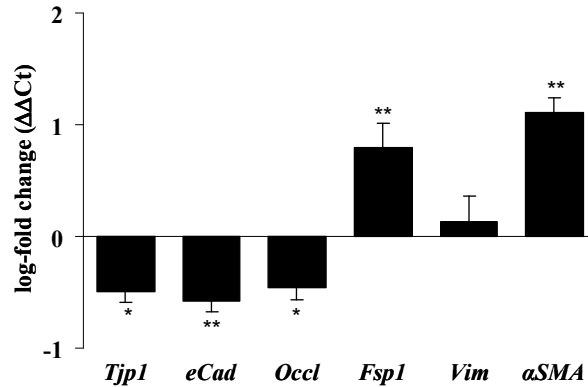
Figure 26. Primary mouse ATII cells were stimulated with WISP1 (1 µg/ml, 12 h) and the mRNA levels of the EMT marker genes *eCad*, *Tjp1*, *Occl*, *Fsp1*, *Vim*, and *αSMA* were analyzed by qRT-PCR (n = 5 for each). All qRT-PCR results are presented as mean ± s.e.m., ** $p < 0.02$, * $p < 0.05$.

The induction of EMT was corroborated by immunofluorescent staining, revealing an increase in αSMA positive cells (Figure 27, left panel), as well as αSMA and TJP1 double-positive cells (middle panel) in response to WISP1. This was abrogated by neutralizing antibodies against WISP1 (right panel).
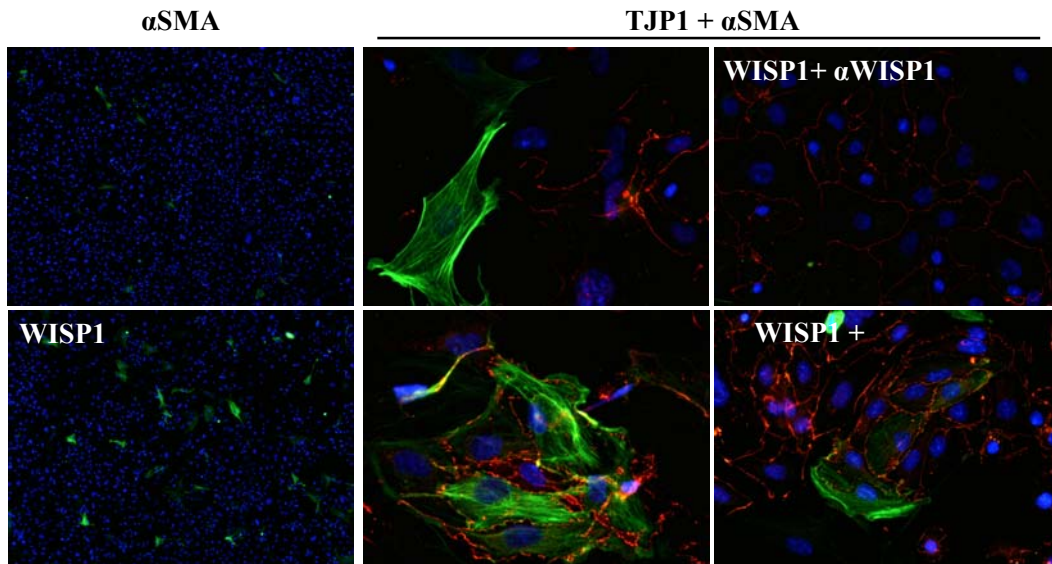
Figure 27. Primary ATII cells were stimulated with WISP1 (1 µg/ml, 12 h) in the absence or presence of neutralizing αWISP1 antibodies or pre-immune serum (IgG control), as indicated. EMT was assessed by immunofluorescent detection of αSMA expression (left panels, original magnification: 10×) and co-localization of αSMA (green) and TJP1 (red) (middle and right panels, original magnification: 40×). Nuclei were visualized by DAPI staining.

Furthermore, treatment with WISP1 lead to enhanced migration of ATII cells, which is associated with the process of EMT (Figure 28A). WISP1 treatment of ATII cells rapidly induced the expression of pro-migratory genes, such as *Mmp7* and *Mmp9*, as well as the previously identified mediators in pulmonary fibrosis, such as *Pai1*, and *Spp1* (Figure 28B). This strongly suggests that WISP1 is not only causally involved in ATII cell hyperplasia, but also induces increased expression and secretion of profibrotic mediators, thereby further perpetuating the process of lung fibrosis. Finally, the potential of ATII cells to undergo EMT *in vivo* was supported by qRT-PCR analysis of freshly isolated ATII cells, which revealed a gain of mesenchymal marker expression and a loss in epithelial cell marker expression in ATII cells isolated from fibrotic mouse lungs (Figure 28C).
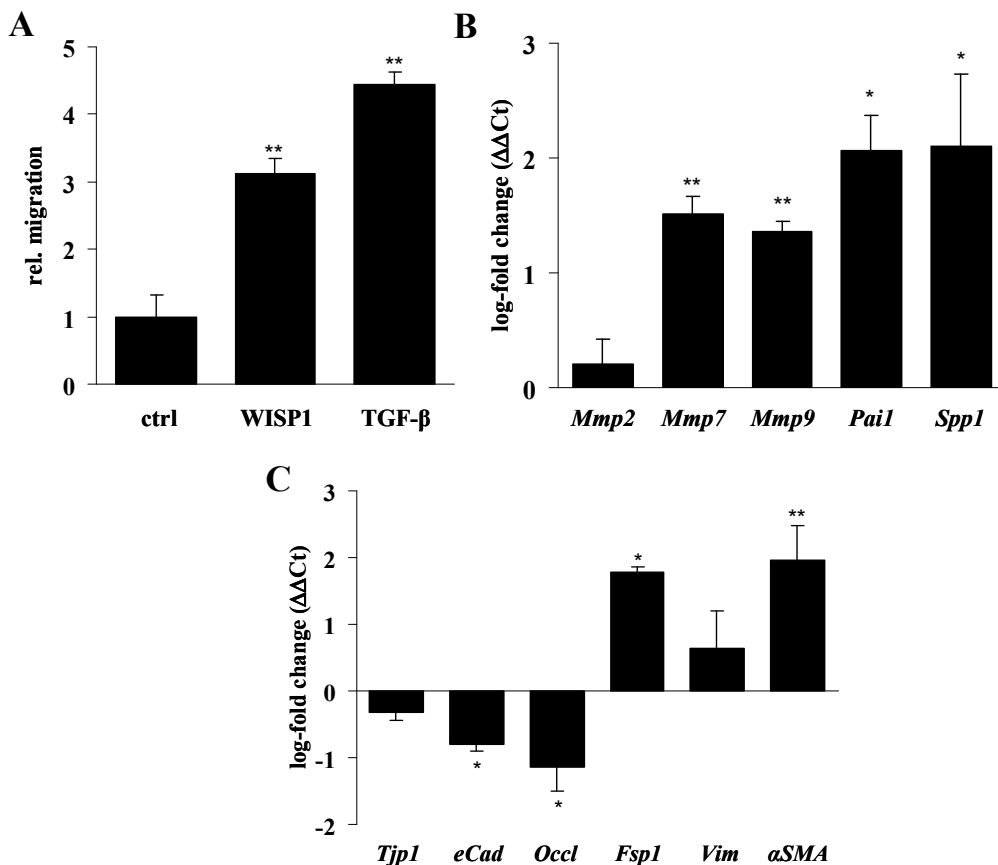
Figure 28. (**A**) The migration of ATII cells in response to WISP1 was determined in a Boyden Chamber assay, TGF-β1 (2 ng/ml) was used as a positive control. Data are presented as the mean ± s.e.m. (n = 6). (**B**) Primary ATII cells were stimulated with WISP1 (1 µg/ml, 12 h) and the mRNA levels of *Mmp2*, *Mmp7*, *Mmp9*, and *Pai1* and *Spp1* were analyzed by qRT-PCR (n = 5 each). (**C**) The mRNA levels of the EMT marker genes *eCad*, *Tjp1*, *Occl*, *Fsp1*, *Vim*, and *αSMA* were determined by qRT-PCR in primary ATII cells isolated from saline- or bleomycin-treated mice 14 d after administration (n = 6).

Attenuation of lung fibrosis in vivo by WISP1 inhibition

To assess whether modulation of WISP1 activity represented an effective therapeutic option in lung fibrosis, we depleted WISP1 during bleomycin-induced lung fibrosis using antibodies shown to be effective in neutralizing WISP1 activity (Figure 24 and 27). To this extent, mice were subjected to bleomycin-induced lung fibrosis, and treated with repetitive orotracheal applications of αWISP1, or species-matched pre-immune control antibodies. Mice subjected to WISP1 neutralization exhibited significantly less pulmonary fibrosis and a marked decrease in ECM deposition, as assessed by quantification of total lung collagen (bleo + IgG: 295 ± 17% vs. bleo + αWISP1: 160 ± 31%, compared with saline-treated controls) (Figure 29), immunohistochemistry for type 1 collagen (Figure 30), as well as αSMA immunostaining (Figure 31).
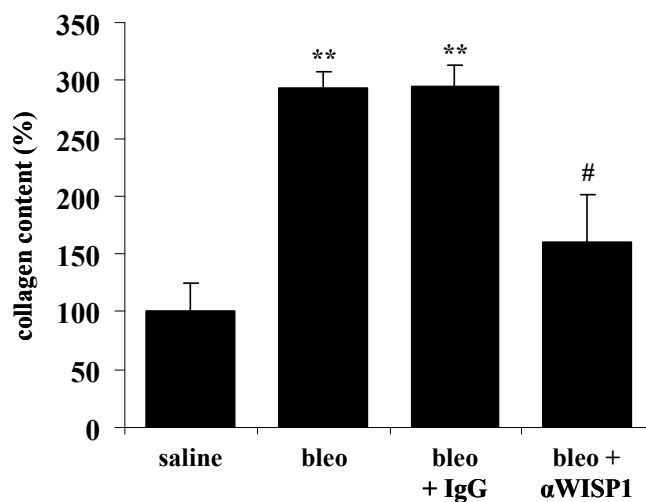
Figure 29. Total collagen content in lung homogenates was quantified using the Sircol collagen assay. Results are derived from whole lungs harvested 14 days after saline, bleomycin, bleomycin plus pre-immune serum (IgG control), or bleomycin plus neutralizing αWISP1 antibody instillation by orotracheal application, as indicated (n = 5 each). Results are presented as mean ±.s.e.m., ** $p<0.02$, # $p<0.02$ vs. bleo + IgG.

bleo

bleo + αWISP1　　　　**bleo + IgG**
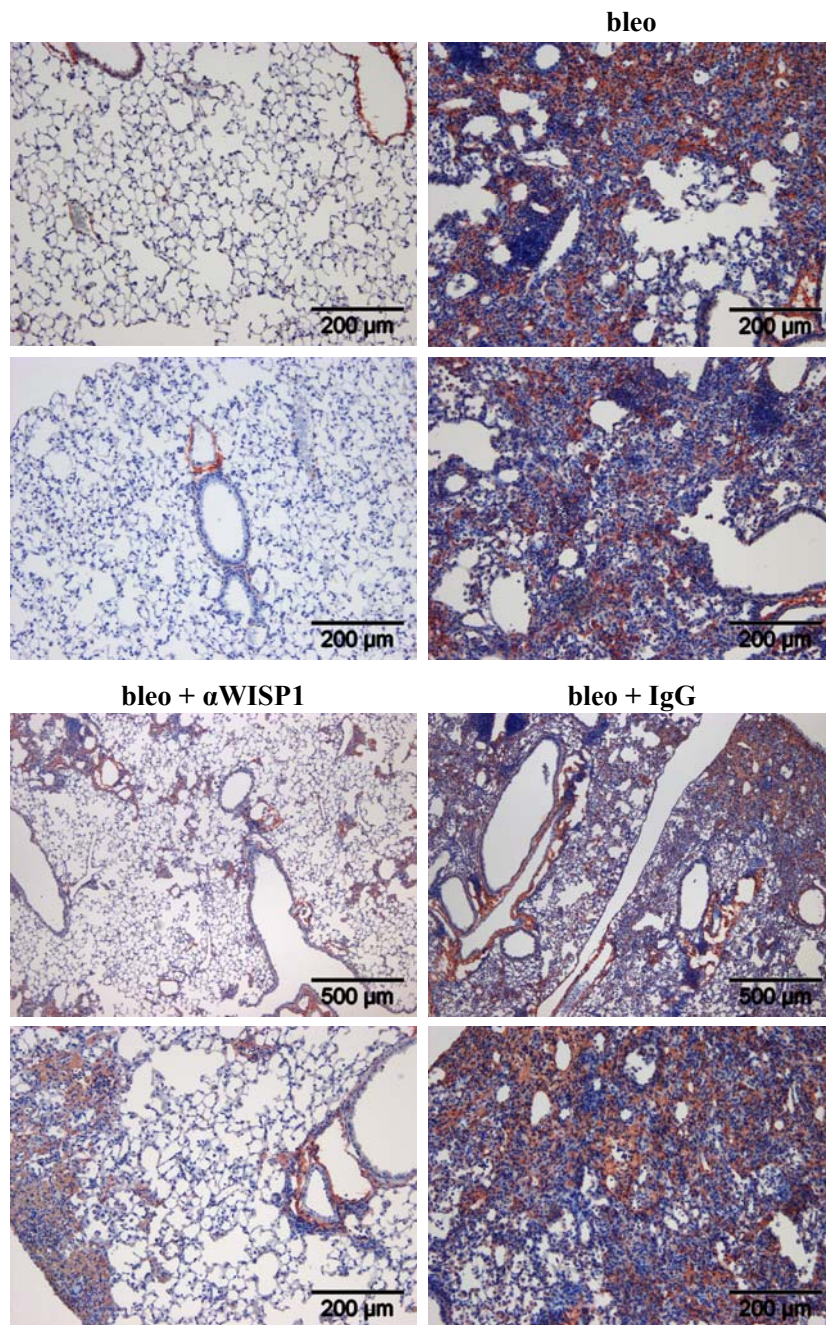
Figure 30. Mice were subjected to saline or bleomycin instillation, as described before, and treated either with neutralizing αWISP1 antibodies or pre-immune serum (IgG control) by orotracheal application as described in detail in *Material & Methods*. Lungs were processed 14 d after bleomycin application for immunohistochemical analysis and stained for type I collagen.

saline   **bleo**

bleo + αWISP1   **bleo + IgG**
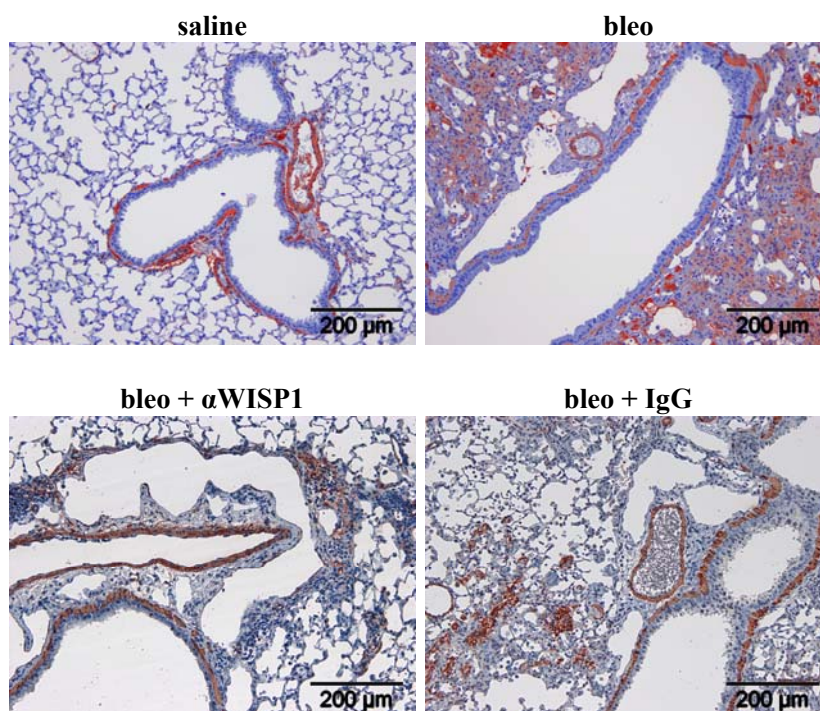
Figure 31. Indicated lung sections were used for immunohistochemical analysis and stained with αSMA. Pictures are representative of at least two independent experiments using at least four different lung tissues for each condition.

These findings were corroborated by the fact that WISP1 neutralization also led to decreased mRNA expression of the profibrotic markers *Col1a1*, *Spp1*, *Mmp7*, and *Pai1* (Figure 32A), which is of significance as we have shown that WISP1 induces the expression of these markers in primary ATII cells (Figure 28B). In addition, WISP1 neutralization resulted in a reversal of EMT marker gene expression *in vivo* (Figure 32B), which were induced by WISP1 *in vitro* (Figure 26).

A

B
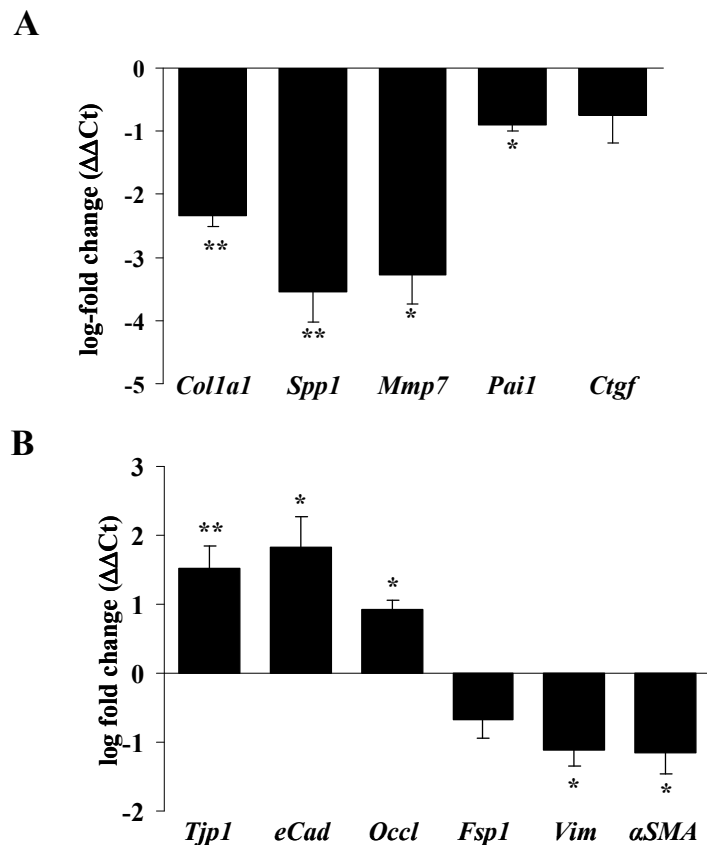
Figure 32. The mRNA levels of the profibrotic marker genes *Col1a1*, *Spp1*, *Mmp7*, *Pai1*, and *Ctgf* (**A**), and the EMT marker genes *Tjp1*, *eCad*, *Occl*, *Fsp1*, *Vim*, and *αSMA* (**B**) were analyzed by qRT-PCR (n = 5 each). Results are plotted as log-fold change (ΔΔCt) of mRNA levels in lung specimens 14 days after bleomycin instillation treated with neutralizing αWISP1 antibodies, compared with lungs treated with pre-immune serum (IgG control). Results are presented as mean ± s.e.m., * $p < 0.05$, ** $p<0.02$, # $p<0.02$ vs. bleo + IgG treatment. See Figure S6A and S6B in the *supplementary material* for a comparison of all treatment groups.

Finally, WISP1 neutralization partially restored normal lung function, as assessed by lung compliance measurements (bleo ± IgG: 0.065 ± 0.073 ml/kPa vs. bleo ± αWISP1: 0.09 ± 0.11 ml/kPa, 95% C.I., Figure 33A). Most importantly, WISP1 neutralization significantly improved the survival of bleomycin-challenged mice (bleo + IgG: 47% vs. bleo + αWISP1: 74%, n =18 for each) (Figure 33B), presenting as a valuable novel approach for the treatment of lung fibrosis.
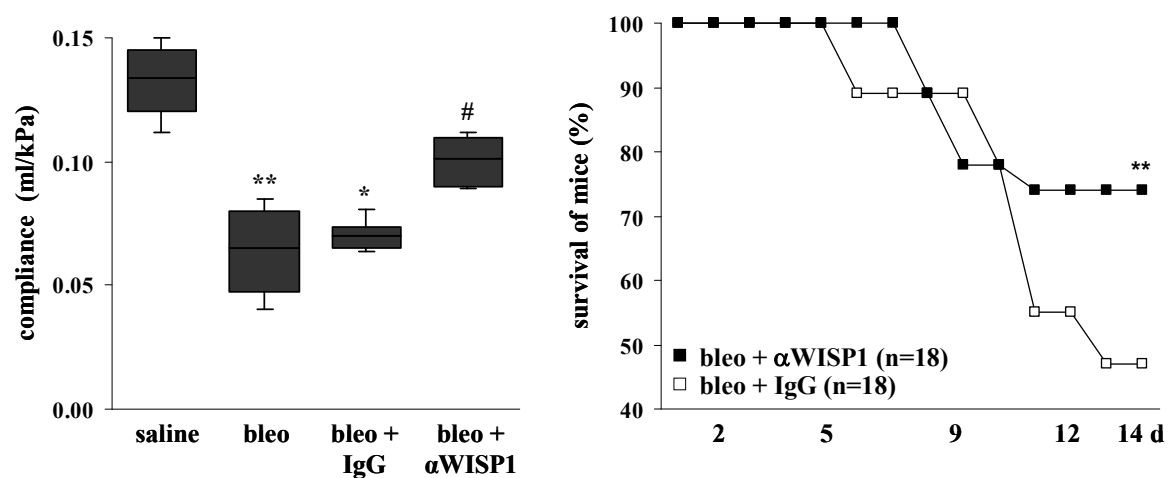
Figure 33. (**A**) Lung compliance measurements were obtained from mice instilled with saline, bleomycin, bleomycin plus IgG control, or bleomycin plus αWISP1 antibody (n = 10 for each), 14 d after initial exposure to bleomycin. *p<0.05, **p<0.02, # p<0.02 vs. bleo + IgG treatment. (**B**) The survival of mice subjected to neutralizing αWISP1 or pre-immune serum (IgG control) instillations (n = 18 for each) was monitored. Days of antibody instillations are indicated on the x-axis, **p<0.02.

DISCUSSION

In the current study, we report that WISP1, a member of the CCN family of secreted cysteine-rich matricellular proteins, represents a novel mediator of impaired epithelial-mesenchymal crosstalk in lung fibrosis and a suitable therapeutic target in this disease. We demonstrated that WISP1 was highly expressed in hyperplastic ATII cells, mediated enhanced ATII cell proliferation, and induced profibrotic marker gene expression in ATII cells. In addition, WISP1 enhanced fibrogenesis by inducing EMT of ATII cells, indicating that WISP1 exerts its profibrotic effects by a multitude of effects in the lung (Figure 36). Most importantly, neutralization of WISP1 resulted in marked attenuation of bleomycin-induced lung fibrosis.

These findings are of special interest, as IPF exhibits a poor prognosis due to unresponsiveness to currently available therapies. IPF is the most common form of idiopathic interstitial pneumonias (IIP), which all exhibit distortion of normal tissue architecture and a loss of lung function (1, 69). This fibrotic tissue transformation is characterized by an increase in total lung collagen levels with the inability of the lung to properly conduct gas exchange. While historically, inflammatory processes were thought to trigger and facilitate the progression of IPF (69, 70), this view has recently been questioned, primarily due to the ineffectiveness of anti-inflammatory therapy in IPF (28, 71). A major key pathophysiological event in IPF that is currently discussed includes repetitive alveolar epithelial cell injury and stimulation without appropriate repair and subsequent fibroblast activation (28, 72).

Alveolar epithelial cell proliferation in IPF

At the onset of our studies, we sought to define alterations in the phenotype and gene expression profile of ATII cells that may initiate and perpetuate the progression of lung fibrosis. The findings that ATII cells from fibrotic lungs exhibited an increased proliferative capacity and enhanced gene expression of proliferative mediators indicated to us that ATII cell proliferation is a dominant pathophysiologic mechanism after initial injury in experimental lung fibrosis.

Indeed, injury and apoptosis within the alveolar epithelium, with subsequent ATII cell hyperplasia, are consistent findings in experimental and human lung fibrosis. In human lung biopsies, nascent fibrotic foci colocalize with unrepaired or abnormal epithelia (73). In addition, experimental delay of epithelial repair in animal models of lung injury facilitates subsequent fibrogenesis (74).

Several studies reported epithelial apoptosis occuring in experimental lung fibrosis (75-77) and human IPF lungs (78-81). Exogenous induction of epithelial apoptosis, e.g. by intratracheal application of Fas ligand, has been reported to lead to lung fibrosis (82). Moreover, inhibition of epithelial apoptosis attenuated experimental lung fibrosis (77). Causality between apoptosis and the fibrogenic process, however, still remains unclear (30, 83). Most interestingly, epithelial hyperplasia and proliferation is reported as well in both experimental lung fibrosis (84, 85) and IPF (86, 87, 88). Ultrastructural studies have revealed the existence of proliferative alveolar epithelial cells immediately adjacent to injured epithelial cells (89-91), suggesting that epithelial apoptosis and proliferation and hyperplasia occur simultaneously during the process of fibrosis. It is, however, unclear whether increased apoptosis and/or proliferation of ATII cells represent the initial trigger for enhanced ECM deposition in lung fibrosis (28, 29, 86).

With respect to the finding of hyperplastic, proliferating alveolar epithelial cells in pulmonary fibrosis, it has to be highlighted that an increased incidence of lung cancer in IPF suggests a link between epithelial cell hyperplasia, impaired repair, and carcinogenesis (92-94).

The WNT target WISP1 in IPF

One of the most important decisions following a microarray screen of diseased tissues/cells is the choice of the gene of interest for functional intervention studies. Of all genes differentially expressed in fibrotic ATII cells, we focused our study on further delineating WISP1 function in lung fibrosis for the following reasons:

First, WISP1 is reported to be a WNT target and WNT signalling is essential to organ development, a process that is recapitulated in organ failure (62, 87, 95,

96). Several WNT ligands, receptors, and components of the canonical pathway are expressed in a highly cell-specific fashion in the developing lung. For instance, WNT2 is highly expressed in the distal mesenchyme (97), while WNT7b is expressed predominantly in the epithelium (98). In addition, WNT5a is expressed in both cell types (99). Active WNT signalling in lung development has also been demonstrated using transgenic WNT reporter mice and nuclear β-catenin staining. TOPGAL or BATGAL mice, both of which harbor a β-galactosidase gene under the control of a LEF/TCF inducible promoter fragment, revealed active canonical WNT signalling early throughout the epithelium and the mesenchyme adjacent to proximal airways at E10.5 - 12.5, which disappeared first in the mesenchyme and was subsequently reduced in the epithelium at E13.5 – E18.5 (100-102). Epithelial-cell specific expression of constitutively active β-catenin leads to epithelial cell dysplasia and ectopic differentiation of alveolar epithelial type II cells in the conducting airways during embryonic development. Postnatally, these mice exhibit air space enlargement and develop pulmonary tumors (102). Lung epithelial cell-specific deletion of β-catenin, in contrast, results in disruption of branching morphogenesis with distorted differentiation of the peripheral lung. The mice died neonatally due to respiratory failure (101).

Second, we and others demonstrated that the WNT/β-catenin pathway is expressed and operative in adult lung epithelium in IPF (87, 103): Chilosi *et al*. reported nuclear localization of β-catenin in ATII cells and interstitial fibroblasts in IPF lungs (87), indicative of activated WNT signalling (104). In addition, we have recently reported that canonical WNT signalling components (including WNT ligands, β-catenin, or GSK-3β) localized mainly to the bronchial and alveolar epithelium in IPF, as observed by immunohistochemistry and gene expression analysis of primary human ATII cells (103). Importantly, an increased activity of the WNT pathway in IPF was documented by increased phosphorylation of LRP6 and GSK-3β, which has recently been demonstrated to be a sensitive indicator of WNT activity in tissue sections (105, 106).

Third, WISP1 regulation was previously reported in microarray lists derived from IPF lung homogenates, indicating that WISP1 is consistently upregulated in IPF lung tissues from different cohorts (56, 58). Selman and colleagues have also identified WISP1 to be regulated in a microarray analysis comparing IPF specimen with hypersensitivity pneumonitis (56). Notably, Lewis *et al*. provided a comparison of the gene expression profile of up to 12 different mouse models of infection, allergy, and lung injury (107). The authors reported regulation of WISP1 in the mouse model of bleomycin-induced lung fibrosis, but not in any other inflammatory models (107).

Fourth, increased WISP1 expression has been shown to be causally involved in epithelial cell hyperplasia in breast cancer cell lines (108). Finally, recent evidence has suggested that WISP1 exhibited anti-apoptotic and proliferative effects on epithelial as well as mesenchymal cell lines (109, 110) and its mRNA expression is associated with non small cell lung carcinoma lung cancer (111). In addition, several WNT proteins are overexpressed in non small cell lung carcinoma, including WNT1 and WNT2, and cancer cells expressing WNT1 or WNT2 are resistant to apoptotic therapies (112, 113).

Role of WISP1 in alveolar epithelial cell function

In our current study, we present *in vitro* and *in vivo* evidence demonstrating that WISP1 acted as a proliferative mediator of ATII cells in vitro and localized to hyperplastic ATII cells in vivo. These data are in agreement with recent reports showing a proliferative effect of WISP1 on epithelial cell lines (108, 114). Further, these data, together with the described findings in lung carcinoma specimen, indicate active WNT signalling as a common molecular mechanism linking alveolar epithelial cell transformation and hyperplasia with fibrosis or cancer.

Further, we could show that WISP1 acted in an autocrine fashion by increasing the release of profibrotic cytokines from the alveolar epithelium, including SPP1, MMP7, MMP9, and PAI1. In particular, MMP7 has recently been assigned a key role in pulmonary fibrosis and shown to be expressed in ATII cells (115, 116). In this study, we demonstrated that MMP7, along with SPP1, PAI1, and MMP9

expression is induced by WISP1, essentially suggesting that a plethora of profibrotic markers released from ATII cells in fibrosis is under transcriptional control of WISP1. MMP7 and SPP1 were one of the first genes identified in IPF lungs using oligonucleotide microarrays, and both proteins have been co-localized in hyperplastic alveolar epithelial cells in IPF (55, 115). Furthermore, MMP7-null mice as well as SPP1-null mice developed less lung fibrosis after bleomycin challenge (115, 117). MMP7 is a matrix metalloprotease involved in multiple local inflammatory effects, which has been demonstrated to be explicitly upregulated in IPF compared with hypersensitive pneumonitis or chronic obstructive pulmonary disease (116). MMP7, along with MMP1, has been demonstrated to be significantly increased in plasma, serum, and bronchoalveolar lavage fluid from IPF patients. In combination, blood levels of MMP1 and MMP7 may be used to distinguish IPF from hypersensitive pneumonitis, thereby representing as potential peripheral blood biomarkers (116).

Interestingly, MMP7 is able to cleave and thereby activate SPP1 (118). SPP1, a secreted glycoprotein, increases the migration and proliferation of fibroblasts and alveolar epithelial cells (55). SPP1-null mice exhibited an attenuated response to bleomycin with reduced type I collagen expression and TGF-β activity (117). Likewise WISP1, MMP7 and SPP1 are both β-catenin target genes (119-121), which further corroborate that active WNT/β-catenin signalling is involved in the development and progression of experimental as well as idiopathic pulmonary fibrosis. Our finding that WISP1 induce MMP7 and SPP1 expression, indicate a possible positive feedback role for WISP1, further potentiating the profibrotic effects triggered by WNT/β-catenin signalling.

PAI1 is a direct TGF-β target, known to be upregulated in different models of lung fibrosis (122-124). TGF-β has been identified has a clear pathogenic growth factor in experimental and idiopathic pulmonary fibrosis (44, 68, 125-128). Studies in transgenic animals with a lung tissue–specific expression of TGF-β as well as adenoviral-mediated epithelial overexpression demonstrated that the presence of active TGF-β induce fibrotic alterations, increased matrix deposition,

and parenchymal tissue distortion. It has been demonstrated that TGF-β1 induces PAI1 expression, which leads to an inhibition of plasminogen activation (122). This mechanism lead to decreased plasminogen-induced fibroblasts apoptosis and presents a possible role of TGF-β/PAI1 in facilitating (myo)-fibroblast survival in fibrotic diseases (122).

Further studies are needed to reveal the detailed interaction of WISP1 with other profibrotic mediators, as well as distinct signalling pathways involved in WISP1-induced effects. In this respect, we observed the activation of the Akt kinase (Figure 34), which is in line with previous data demonstrating Akt activation in response to WISP1 (109).
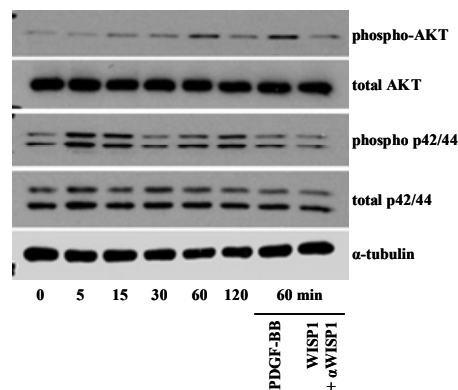
Figure 34. (A) Primary mouse ATII cells were stimulated with WISP1 (1 µg/ml) for the indicated time points. Phosphorylated and total protein of AKT and p44/42 was analyzed by Western Blotting. PDGF served as a positive control.

Role of WISP1 in epithelial - mesenchymal interaction

IPF is considered a disease of impaired epithelial-mesenchymal crosstalk (28, 30), evidenced by the close proximity of hyperplastic and injured alveolar epithelial cells with fibroblast foci (27, 89). The pathological remodeling of lung tissue during disease pathogenesis of IPF can be dictated by direct cellular contact, or, as described in the study herein, the secretion of soluble mediators in an autocrine and/or paracrine fashion. WISP1 expression was increased in lung fibrosis, but its expression was exclusively regulated in alveolar epithelial cells, whereas neither increased mRNA nor protein expression was detectable in fibroblasts derived from experimental lung fibrosis or IPF lungs. Several recent

findings from our group, however, also support a paracrine effect of ATII cell-derived WISP1 on interstitial fibroblasts (Figure 35). We demonstrated that WISP1 led to increased expression of (myo)-fibroblast activation markers and deposition of ECM molecules. While we did not observed an influence of WISP1 on fibroblast proliferation, a recent publication by Colston *et al.* (110) demonstrated a proproliferative effect of WISP1 on cardiac fibroblasts, suggesting a role for WISP1 in the remodeling of myocardial infarction.
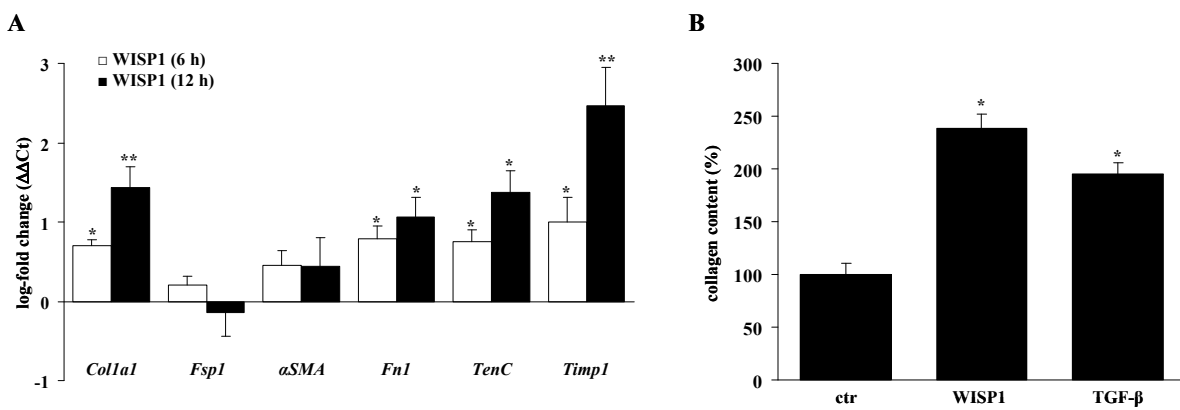
Figure 35. (A) Human lung fibroblasts were stimulated with WISP1 (1 μg/ml; 6 or 12 h, as indicated), and the mRNA levels of the ECM components type I collagen α1 (*Col1a1*), fibronectin (*Fn1*), the (myo)-fibroblast activation markers *Fsp1, αSMA*, tenascin C (*TenC*), and *Timp1* were analyzed by qRT-PCR (n = 3). **(B)** Human lung fibroblasts were stimulated with WISP1 (1 μg/ml) or TGF-β1 (2 ng/ml) for 24 h and total collagen content was quantified using the Sircol collagen assay (n = 3). This Figure is kindly provided by Monika Kramer.

WISP in epithelial-to-mesenchymal transition (EMT)

The hallmark lesions of IPF are fibroblast foci, which are sites featuring activated myofibroblasts, synthesizing and depositing a collagen-rich ECM. The number of smooth muscle actin-positive, activated (myo)-fibroblasts is significantly increased in multiple forms of pulmonary fibrosis including IPF, but their origin remains to be elucidated. Currently, three major theories attempt to explain the origin of interstitial fibroblasts. It has been demonstrated that resident pulmonary fibroblasts can be activated in response to fibrogenic cytokines and growth factors, thereby increasing the fibroblast pool via local fibroproliferation (33). In addition, several recent studies have shown that bone marrow-derived circulating

fibrocytes cells traffic to the lung during experimental lung fibrosis, and serve as progenitors for interstitial fibroblast (35, 36, 129). Third, it was recently proposed that ATII cells are capable of undergoing the process of EMT, the phenotypic, reversible switching of epithelial to fibroblast-like cells, which is initiated by an alteration of the transcriptional and proteomic profile of ATII cells (38, 39). Here, we report that WISP1 led to the induction of EMT by regulation of marker gene expression and induction of ATII cell migration. As TGF-β represents a main inducer of EMT in multiple organ systems (67, 68), further studies are needed to fully appreciate the mechanistical role of WISP1 and its connectivity to the TGF-β pathway in this context.

Role of WISP1 in lung fibrosis

Our study demonstrates impaired epithelial-mesenchymal crosstalk in IPF, and suggests that the auto- and paracrine effects of WISP1, a member of the CCN family of secreted, cysteine-rich regulatory proteins, can initiate and perpetuate the fibrotic process at the interface of ATII cells and interstitial fibroblasts in the lung (Figure 36). Whether WISP1 induces proliferation, EMT and/or ECM deposition *in vivo* is most probably dictated by the ATII cell microenvironment in disease. While an intact subepithelial ECM may facilitate proliferation, a disrupted and/or perturbed ECM will facilitate EMT, as recently suggested in the case of TGF-β (38). WISP1, a signalling molecule downstream of the WNT signalling pathway, has thus far not been assigned a role in pathologies of the lung. Recent evidence, however, suggested that the WNT pathway, which is critical during normal development and morphogenesis, is reactivated in IPF. Future work will undoubtedly shed more light on the molecular mechanisms of WISP1 signalling and its downstream effects in IPF, and the therapeutic options derived thereof.
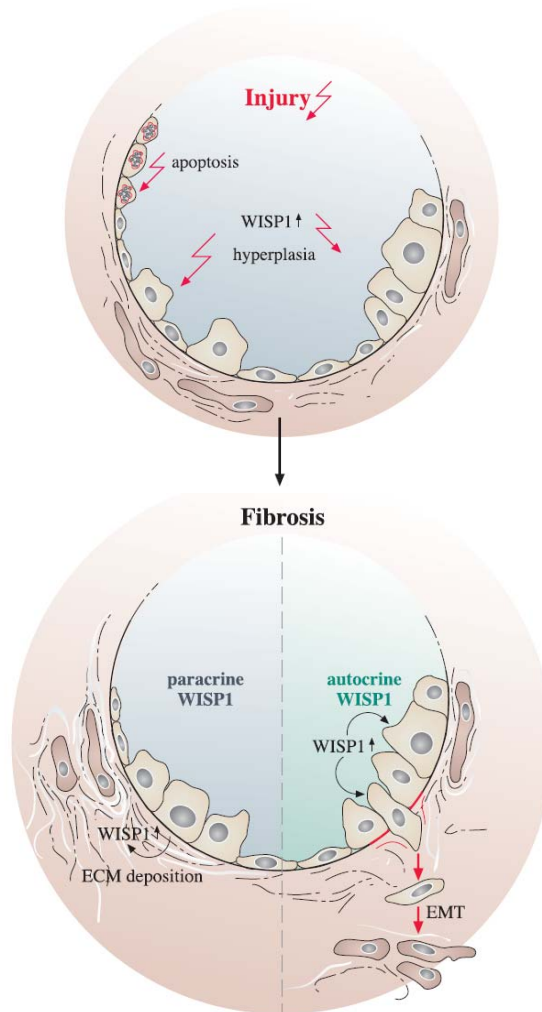
Figure 36. The role of WISP1 in lung fibrosis. A proposed model depicting the role of WISP1 in lung fibrosis is shown. Initial injury leads to increased WISP1 expression by hyperplastic ATII cells, which sustains ATII cell hyperplasia. Fibrogenesis is then promoted via autocrine (lower right part) or paracrine (lower left part) effects on ATII cell mediator release and EMT, and/or fibroblast ECM synthesis, respectively.

SUPPLEMENTARY INFORMATION

Abbreviations

AA	Amino acid
BAL (F)	bronchoalveolar lavage (fluid)
BSA	Bovine serum albumin
cDNA	Complementary deoxyribonucleic acid
CHAPS	3-[3-chloramidopropyl)dimethylammonio]-1-propanesulfonate
DAPI	4´,6-diamidino-2-phenylindole
DMSO	Dimethyl sulfoxide
DTT	Dithiothreitol
ECM	Extracellular matrix
EDTA	Ethylendinitrilo-N,N,$N´,N´$,-tetra-acetate
FITC	Fluorescein-5-isothiocyanate
FCS	Fetal calf serum
HEPES	2-(-4-2-hydroxyethyl)-piperazinyl-1-ethansulfonate
HRP	Horseradish peroxidase
Im	intramuscular
ip	intraperitoneal
IHC	Immunohistochemistry
mAb	monoclonal antibody
OD	Optical density
PBS	Phosphate-buffered saline
PCR	Polymerase chain reaction
qRT-PCR	Quantitative RT-PCR
rpm	rounds per minute
RT	room temperature
RT-PCR	Reverse transcription PCR
SDS	Sodium dodecyl sulfate
TEMED	N,N,N',N'-tetramethyl-ethane-1,2-diamine
WB	Western blotting
Wt	wildtype

Table S1. Characteristics of IPF patients with UIP pattern. VC = vital capacity, TLC = total lung capacity, DL_{CO}/VA = diffusing capacity of the lung for CO per unit of alveolar volume (all in % predicted), $Pa_{O2/CO2}$ = partial pressure of O_2 /CO_2 in the arterial blood.

no.	diagnosis	gender	Age (yr)	VC (%)	DL_{CO}/VA (%)	TLC (%)	O_2 (l/min)	Pa_{O2} (mmHg)	Pa_{CO2} (mmHg)
1	IPF (UIP)	male	63	56%	33%	48%	3	52	33
2	IPF (UIP)	male	62	50%	26%	52%	3	49	38
3	IPF (UIP)	male	58	49%	na	na	na	na	na
4	IPF (UIP)	male	65	59%	20%	42%	3	53	38
5	IPF (UIP)	male	65	59%	20%	42%	4	69	41
6	IPF (UIP)	male	43	48%	27%	51%	na	na	na
7	IPF (UIP)	male	71	40%	24%	46%	na	na	na
8	IPF (UIP)	male	64	59%	22%	52%	2	58	38
9	IPF (UIP)	male	60	51%	18%	49%	2	59	39
10	IPF (UIP)	male	65	51%	20%	66%	2	53	38
11	IPF (UIP)	male	44	47%	25%	55%	2	36	35
12	IPF (UIP)	female	43	40%	na	na	2	54	35
13	IPF (UIP)	female	42	50%	17%	58%	3	52	36
14	IPF (UIP)	female	66	29%	23%	45%	4	56	45
15	IPF (UIP)	female	62	27%	na	48%	4	71	65

Table S2. Primer sequences and amplicon sizes for human tissues. All primer sets worked under identical quantitative PCR cycling conditions with similar efficiencies to obtain simultaneous amplification in the same run. Sequences were taken from GeneBank, all accession numbers are denoted.

Gene	Accession		Sequences (5´ → 3´)	Length	Amplicon
CTGF	NM001901	for	cct gca ggc tag aga agc aga	21bp	103bp
		rev	ttt ggg agt acg gat gca ctt	21bp	
CYR61	NM001554	for	aaa ggc agc tca ctg aag cg	20bp	110bp
		rev	gca ctg gga cca tga agt tgt	21bp	
HPRT1	NM000194	for	aag gac ccc acg aag tgt tg	20bp	157bp
		rev	ggc ttt gta ttt tgc ttt tcc a	22bp	
NOV	NM002514	for	ccg tca atg tga gat gct gaa	21bp	107bp
		rev	ttg gtg cgg aga cac ttt ttt	21bp	
WISP1	NM003882	for	gta tgt gag gac gac gcc aag	21bp	104bp
		rev	ggc tat gca gtt cct gtg cc	20bp	
WISP2	NM003881	for	gac atg aga ggc aca ccg aag	21bp	94bp
		rev	gta cat ggt gtc ggg cac ag	20bp	
WISP3	NM003880	for	ctc cac tct tct gct tgc tgg	21bp	87bp
		rev	agg cct tcc ttc agg tgt tgt	21bp	

Table S3. Primer sequences and amplicon sizes for mouse tissues. All primer sets worked under identical quantitative PCR cycling conditions with similar efficiencies to obtain simultaneous amplification in the same run. Sequences were taken from GeneBank, all accession numbers are denoted.

Gene	Accession		Sequences (5´ → 3´)	Length	Amplicon
β-catenin	NM007614	for	tca aga gag caa gct cat cat tct	24bp	115bp
		rev	cac ctt cag cac tct gct tgt g	22bp	
Cdh16	NM007663	for	tgc aga aag cct gca cac a	19bp	130bp
		rev	tgc cgt gtt tga gtc tcc tg	20bp	
Col1a1	NM007742	for	cca aga aga cat ccc tga agt ca	23bp	128bp
		rev	tgc acg tca tcg cac aca	18bp	
Col1a2	NM007743	for	agc ttt gtg gat acg cgg act	21bp	86bp
		rev	tcg tac tga tcc cga ttg ca	20bp	
Ctgf	NM010217	for	ctt ctg cga ttt cgg ctc c	19p	115bp
		rev	tgc ttt gga agg act cac cg	20bp	
Cyclin G1	NM009831	for	tgg ctg tca aga tga tag aag tac tga	27bp	94bp
		rev	tgg ctg aca tct aga ctc ctg ttc	24bp	
Cyclin B2	NM007630	for	gtc aac aag cag ccg aaa cc	20bp	75bp
		rev	gag gac gat cct tgg gag cta	2qbp	
Cyr61	NM010516	for	cca ccg ctc tga aag gga t	19bp	80bp
		rev	ccc cgt ttt ggt aga ttc tgg	21bp	
Fizz1	NM020509	for	tat gaa cag atg ggc ctc ctg	21bp	90bp
		rev	tcc act ctg gat ctc cca aga	21bp	

Fn	NM010233	for	gtg tag cac aac ttc caa tta cga a	25bp	90bp
		rev	gga att tcc gcc tcg agt ct	20bp	
Fsp1	NM011311	for	agg agc tac tga cca ggg agc t	22bp	102bp
		rev	tca ttg tcc ctg ttg ctg tcc	21bp	
Fzd1	NM021457	for	aaa cag cac agg ttc tgc aaa a	22bp	58bp
		rev	tgg gcc ctc tcg ttc ctt	18bp	
Fzd2	NM020510	for	tcc atc tgg tgg gtg att ctg	21bp	66bp
		rev	ctc gtg gcc cca ctt cat t	19bp	
Fzd3	NM021458	for	gcc tat agc gag tgt tca aaa ctc a	25bp	78bp
		rev	tgg aaa cct act gca ctc cat atc t	25bp	
Fzd4	NM008055	for	gcc cca gaa cga cca caa	18bp	64bp
		rev	ggg caa ggg aac ctc ttc at	20bp	
Gsk3β	NM_019827	for	ttt gag ctg gta ccc tag gat ga	23bp	75bp
		rev	ttc ttc gct ttc cga tgc a	19bp	
Hmbs	NM013551	for	atg tcc ggt aac ggc ggc	22bp	135bp
		rev	ggt aca agg ctt tca gca tcg c	18bp	
Inha	NM008380	for	gga ggg ccg aaa tga atg a	19bp	84bp
		rev	tgc agt gtc ttc ctg gct gt	20bp	
Kcne2	NM134110	for	ggt ctc ctg cat tgc tca cat	21bp	82bp
		rev	cat cct cca gtg tct ggg tca	21bp	
Ki67	NM001081 117	for	ttg acc gct cct tta ggt atg aa	23bp	138bp
		rev	ggt atc ttg acc ttc ccc atc a	22bp	

Lef1	NM010703	for	ggc ggc gtt gga cag at	17bp	67bp
		rev	cac ccg tga tgg gat aaa cag	21bp	
Lrp5	NM008513	for	caa cgt gga cgt gtt tta ttc ttc	24bp	138bp
		rev	cag cga ctg gtg ctg tag tca	21bp	
Lrp6	NM008514	for	cca ttc ctc tca ctg gtg tca a	22bp	146bp
		rev	gcc aaa ctc tac cac atg ttc ca	23bp	
Mmp2	NM008610	for	atc gag acc atg cgg aag c	19bp	123bp
		rev	atc cac ggt ttc agg gtc c	19bp	
Mmp7	NM010810	for	cct agg cgg aga tgc tca ct	20bp	96bp
		rev	gct gcc acc cat gaa ttt g	19bp	
Mmp9	NM01399	for	cgc ctt ggt gta gca caa ca	20bp	106bp
		rev	aca ggg ttt gcc ttc tcc gtt	21bp	
Nov	NM010930	for	aac aac cag act ggc att tgc	21bp	133bp
		rev	cag cca atc tgc cca tct ct	20bp	
Pai1	NM008871	for	gtc ttt ccg acc aag agc ag	20bp	104bp
		rev	gac aaa ggc tgt gga gga ag	20bp	
Sfrp1	NM013834	for	gta caa ccg tgt gtc ctc cat	21bp	89bp
		rev	cat cct cag tgc aaa ctc gct	21bp	
αSMA	NM007392	for	gct ggt gat gat gct ccc a	19bp	80bp
		rev	gcc cat tcc aac cat tac tcc	21bp	
Spp1	NM009263	for	gtt tgg cat tgc ctc ctc c	19bp	83bp
		rev	gga tct ggg tgc agg ctg ta	20bp	

Tcf3	NM009332	for	tcc agc aca ctt gtc caa caa	21bp	61bp
		rev	cag cgg gtg cat gtg atg	18bp	
Tcf4	NM009333	for	gtg gga act gcc ccg ttt	18bp	59bp
		rev	gtt cta aga gca cag ggc agt tg	23bp	
Wisp1	NM018865	for	gtc ctg agg gtg ggc aac at	20bp	97bp
		rev	ggg cgt gta gtc gtt tcc tct	21bp	
Wisp2	NM016873	for	tac agg tgc cag gaa ggt gc	20bp	119bp
		rev	cag atg cag gag tga caa ggg	21bp	
Wisp3	XM282903	for	ggc gtg tgc gca tat ctt g	19bp	98bp
		rev	agg cag ctg aac agt ggg tg	20bp	
Wnt1	NM021279	for	caa atg gca att ccg aaa cc	20bp	112bp
		rev	gat tgc gaa gat gaa cgc tg	20bp	
Wnt2	NM023653	for	agc cct gat gaa cct tca caa c	22bp	78bp
		rev	tga cac ttg cat tct tgt ttc aag	24bp	
Wnt3a	NM009522	for	gca cca ccg tca gca aca	18bp	57bp
		rev	ggg tgg ctt tgt cca gaa ca	20bp	
Wnt7b	NM009528	for	tcg aaa gtg gat ctt tta cgt gtt t	25bp	67bp
		rev	tga caa tgc tcc gag ctt ca	20bp	
Wnt10b	NM011718	for	tgg gac gcc agg tgg taa	18bp	60bp
		rev	ctg acg ttc cat ggc att tg	20bp	

rabbit alexa 488	FITC	rat alexa 555

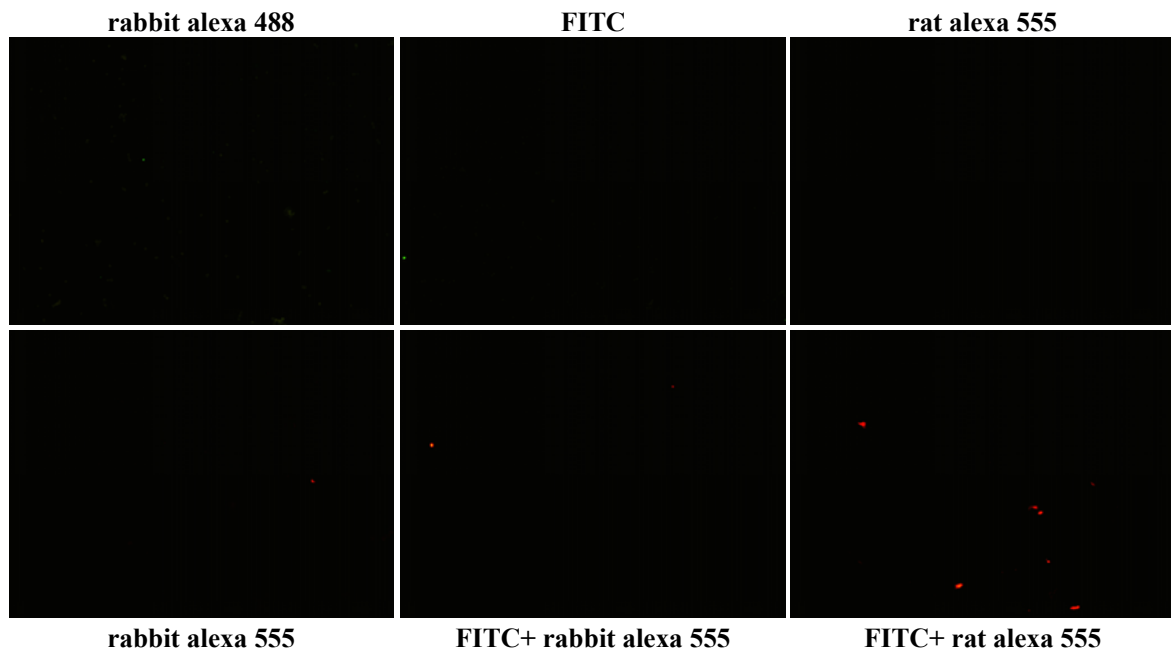| rabbit alexa 555	FITC+ rabbit alexa 555	FITC+ rat alexa 555

Figure S1. Control negative immunostaining for the antibodies used in the study. Cells were prepared as described, irrelevant IgG used in replacement of a specific primary antibody, and secondary antibodies used as indicated (magnification 10×).

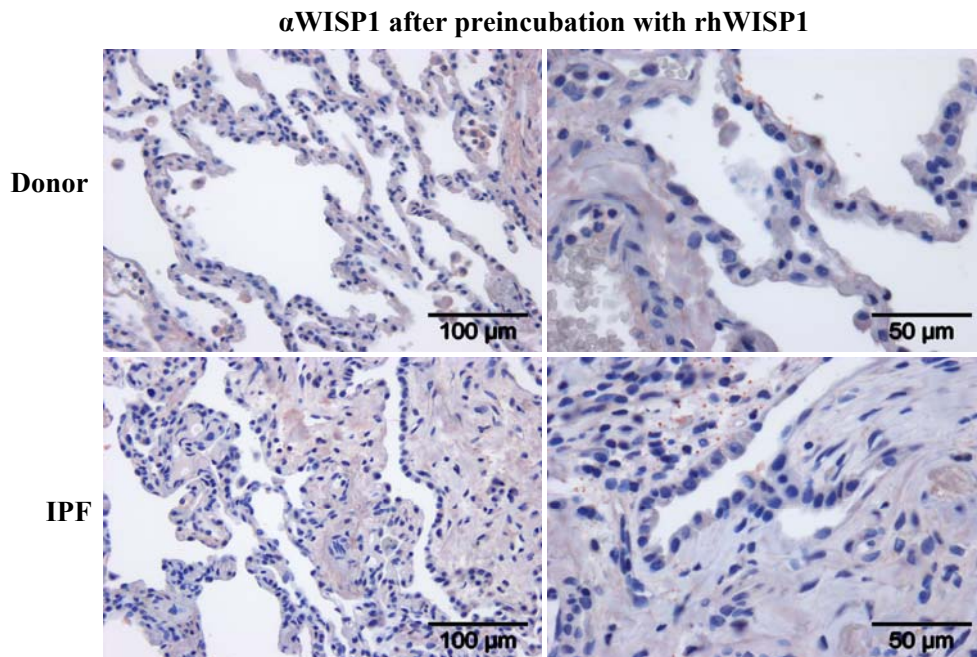**αWISP1 after preincubation with rhWISP1**

Figure S2. Control immunohistochemical staining of sections from control (transplant donor) or IPF lung tissue specimen for the WISP1 antibody used in Figure 6D and 6E. The antibody was preincubated with recombinant human WISP1 protein before processing.

REFERENCES

1. American Thoracic Society/European Respiratory Society international multidisciplinary consensus classification of the idiopathic interstitial pneumonias. *AJRCCM* 2002;165(2):277-304.

2. Martinez FJ, Safrin S, Weycker D, Starko KM, Bradford WZ, King TE, Jr., Flaherty KR, Schwartz DA, Noble PW, Raghu G, et al. The clinical course of patients with idiopathic pulmonary fibrosis. *Ann Intern Med* 2005;142(12 Pt 1):963-967.

3. Taskar VS, Coultas DB. Is idiopathic pulmonary fibrosis an environmental disease? *Proc Am Thorac Soc* 2006;3(4):293-298.

4. Collard HR, Moore BB, Flaherty KR, Brown KK, Kaner RJ, King TE, Jr., Lasky JA, Loyd JE, Noth I, Olman MA, et al. Acute exacerbations of idiopathic pulmonary fibrosis. *AJRCCM* 2007;176(7):636-643.

5. Gharaee-Kermani M, Hu B, Thannickal VJ, Phan SH, Gyetko MR. Current and emerging drugs for idiopathic pulmonary fibrosis. *Expert Opin Emerg Drugs* 2007;12(4):627-646.

6. Walter N, Collard HR, King TE, Jr. Current perspectives on the treatment of idiopathic pulmonary fibrosis. *Proc Am Thorac Soc* 2006;3(4):330-338.

7. Swigris JJ, Brown KK. Acute interstitial pneumonia and acute exacerbations of idiopathic pulmonary fibrosis. *Semin Respir Crit Care Med* 2006;27(6):659-667.

8. Swigris JJ, Kuschner WG, Jacobs SS, Wilson SR, Gould MK. Health-related quality of life in patients with idiopathic pulmonary fibrosis: A systematic review. *Thorax* 2005;60(7):588-594.

9. Noble PW. Idiopathic pulmonary fibrosis: Natural history and prognosis. *Clin Chest Med* 2006;27(1 Suppl 1):S11-16, v.

10. Dempsey OJ. Clinical review: Idiopathic pulmonary fibrosis--past, present and future. *Respir Med* 2006;100(11):1871-1885.

11. Swigris JJ, Kuschner WG, Kelsey JL, Gould MK. Idiopathic pulmonary fibrosis: Challenges and opportunities for the clinician and investigator. *Chest* 2005;127(1):275-283.

12. Nathan SD. Therapeutic management of idiopathic pulmonary fibrosis: An evidence-based approach. *Clin Chest Med* 2006;27(1 Suppl 1):S27-35, vi.

13. Antoniu SA. Pirfenidone for the treatment of idiopathic pulmonary fibrosis. *Expert Opin Investig Drugs* 2006;15(7):823-828.

14. Bouros D, Antoniou KM, Tzouvelekis A, Siafakas NM. Interferon-gamma 1b for the treatment of idiopathic pulmonary fibrosis. *Expert Opin Biol Ther* 2006;6(10):1051-1060.

15. Demedts M, Behr J, Buhl R, Costabel U, Dekhuijzen R, Jansen HM, MacNee W, Thomeer M, Wallaert B, Laurent F, et al. High-dose acetylcysteine in idiopathic pulmonary fibrosis. *N Engl J Med* 2005;353(21):2229-2242.

16. Maher TM, Wells AU. Optimal treatment for idiopathic pulmonary fibrosis. *Thorax* 2008;63(12):1120-1121; author reply 1121.

17. Williams TJ, Wilson JW. Challenges in pulmonary fibrosis: 7--novel therapies and lung transplantation. *Thorax* 2008;63(3):277-284.

18. Daniels CE, Ryu JH. Treatment of idiopathic pulmonary fibrosis. *Semin Respir Crit Care Med* 2006;27(6):668-676.

19. Flaherty KR, Thwaite EL, Kazerooni EA, Gross BH, Toews GB, Colby TV, Travis WD, Mumford JA, Murray S, Flint A, et al. Radiological versus histological diagnosis in uip and nsip: Survival implications. *Thorax* 2003;58(2):143-148.

20. Noth I, Martinez FJ. Recent advances in idiopathic pulmonary fibrosis. *Chest* 2007;132(2):637-650.

21. Maher TM, Wells AU, Laurent GJ. Idiopathic pulmonary fibrosis: Multiple causes and multiple mechanisms? *Eur Respir J* 2007;30(5):835-839.

22. du Bois RM. Evolving concepts in the early and accurate diagnosis of idiopathic pulmonary fibrosis. *Clin Chest Med* 2006;27(1 Suppl 1):S17-25, v-vi.

23. Suh RD, Goldin JG. High-resolution computed tomography of interstitial pulmonary fibrosis. *Semin Respir Crit Care Med* 2006;27(6):623-633.

24. White ES, Lazar MH, Thannickal VJ. Pathogenetic mechanisms in usual interstitial pneumonia/idiopathic pulmonary fibrosis. *J Pathol* 2003;201(3):343-354.

25. King TE, Jr., Schwarz MI, Brown K, Tooze JA, Colby TV, Waldron JA, Jr., Flint A, Thurlbeck W, Cherniack RM. Idiopathic pulmonary fibrosis: Relationship between histopathologic features and mortality. *AJRCCM* 2001;164(6):1025-1032.

26. Visscher DW, Myers JL. Histologic spectrum of idiopathic interstitial pneumonias. *Proc Am Thorac Soc* 2006;3(4):322-329.

27. Katzenstein AL, Myers JL. Idiopathic pulmonary fibrosis: Clinical relevance of pathologic classification. *AJRCCM* 1998;157(4 Pt 1):1301-1315.

28. Selman M, King TE, Pardo A. Idiopathic pulmonary fibrosis: Prevailing and evolving hypotheses about its pathogenesis and implications for therapy. *Ann Intern Med* 2001;134(2):136-151.

29. Strieter RM. Pathogenesis and natural history of usual interstitial pneumonia: The whole story or the last chapter of a long novel. *Chest* 2005;128(5 Suppl 1):526S-532S.

30. Horowitz JC, Thannickal VJ. Epithelial-mesenchymal interactions in pulmonary fibrosis. *Semin Respir Crit Care Med* 2006;27(6):600-612.

31. Nicholson AG, Fulford LG, Colby TV, du Bois RM, Hansell DM, Wells AU. The relationship between individual histologic features and disease progression in idiopathic pulmonary fibrosis. *AJRCCM* 2002;166(2):173-177.

32. Hinz B, Phan SH, Thannickal VJ, Galli A, Bochaton-Piallat ML, Gabbiani G. The myofibroblast: One function, multiple origins. *Am J Path* 2007;170(6):1807-1816.

33. Phan SH. Fibroblast phenotypes in pulmonary fibrosis. *AJRCMB* 2003;29(3 Suppl):S87-92.

34. Scotton CJ, Chambers RC. Molecular targets in pulmonary fibrosis: The myofibroblast in focus. *Chest* 2007;132(4):1311-1321.

35. Hashimoto N, Jin H, Liu T, Chensue SW, Phan SH. Bone marrow-derived progenitor cells in pulmonary fibrosis. *J Clin Invest* 2004;113(2):243-252.

36. Phillips RJ, Burdick MD, Hong K, Lutz MA, Murray LA, Xue YY, Belperio JA, Keane MP, Strieter RM. Circulating fibrocytes traffic to the lungs in response to cxcl12 and mediate fibrosis. *J Clin Invest* 2004;114(3):438-446.

37. Moore BB, Murray L, Das A, Wilke CA, Herrygers AB, Toews GB. The role of ccl12 in the recruitment of fibrocytes and lung fibrosis. *AJRCMB* 2006 Aug;35(2):175-81. Epub 2006 Mar 16.

38. Kim KK, Kugler MC, Wolters PJ, Robillard L, Galvez MG, Brumwell AN, Sheppard D, Chapman HA. Alveolar epithelial cell mesenchymal transition develops in vivo during pulmonary fibrosis and is regulated by the extracellular matrix. *Proceedings of the National Academy of Sciences of the United States of America* 2006;103(35):13180-13185.

39. Willis BC, Liebler JM, Luby-Phelps K, Nicholson AG, Crandall ED, du Bois RM, Borok Z. Induction of epithelial-mesenchymal transition in alveolar epithelial cells by transforming growth factor-beta1: Potential role in idiopathic pulmonary fibrosis. *Am J Path* 2005;166(5):1321-1332.

40. Lee JM, Dedhar S, Kalluri R, Thompson EW. The epithelial-mesenchymal transition: New insights in signaling, development, and disease. *J Cell Biol* 2006;172(7):973-981.

41. Thiery JP, Sleeman JP. Complex networks orchestrate epithelial-mesenchymal transitions. *Nat Rev Mol Cell Biol* 2006;7(2):131-142.

42. Willis BC, Dubois RM, Borok Z. Epithelial origin of myofibroblasts during fibrosis in the lung. *Proc Am Thorac Soc* 2006;3(4):377-382.

43. Strieter RM, Gomperts BN, Keane MP. The role of cxc chemokines in pulmonary fibrosis. *J Clin Invest* 2007;117(3):549-556.

44. Sime PJ, Xing Z, Graham FL, Csaky KG, Gauldie J. Adenovector-mediated gene transfer of active transforming growth factor-beta1 induces prolonged severe fibrosis in rat lung. *J Clin Invest* 1997;100(4):768-776.

45.   Konigshoff M, Wilhelm A, Jahn A, Sedding D, Amarie OV, Eul B, Seeger W, Fink L, Gunther A, Eickelberg O, et al. The angiotensin ii receptor 2 is expressed and mediates angiotensin ii signaling in lung fibrosis. *Am J Respir Cell Mol Biol* 2007;37(6):640-650.

46.   Wang R, Ibarra-Sunga O, Verlinski L, Pick R, Uhal BD. Abrogation of bleomycin-induced epithelial apoptosis and lung fibrosis by captopril or by a caspase inhibitor. *AJP* 2000;279(1):L143-151.

47.   Kolb M, Margetts PJ, Anthony DC, Pitossi F, Gauldie J. Transient expression of il-1beta induces acute lung injury and chronic repair leading to pulmonary fibrosis. *J Clin Invest* 2001;107(12):1529-1536.

48.   Gharaee-Kermani M, Gyetko MR, Hu B, Phan SH. New insights into the pathogenesis and treatment of idiopathic pulmonary fibrosis: A potential role for stem cells in the lung parenchyma and implications for therapy. *Pharma Res* 2007;24(5):819-841.

49.   Ask K, Martin GE, Kolb M, Gauldie J. Targeting genes for treatment in idiopathic pulmonary fibrosis: Challenges and opportunities, promises and pitfalls. *Proc Am Thorac Soc* 2006;3(4):389-393.

50.   DasGupta R, Fuchs E. Multiple roles for activated lef/tcf transcription complexes during hair follicle development and differentiation. *Development* 1999;126(20):4557-4568.

51.   Corti M, Brody AR, Harrison JH. Isolation and primary culture of murine alveolar type ii cells. *AJRCMB* 1996;14(4):309-315.

52.   Frank J, Roux J, Kawakatsu H, Su G, Dagenais A, Berthiaume Y, Howard M, Canessa CM, Fang X, Sheppard D, et al. Transforming growth factor-beta1 decreases expression of the epithelial sodium channel alphaenac and alveolar epithelial vectorial sodium and fluid transport via an erk1/2-dependent mechanism. *The Journal of biological chemistry* 2003;278(45):43939-43950.

53.   Fink L, Seeger W, Ermert L, Hanze J, Stahl U, Grimminger F, Kummer W, Bohle RM. Real-time quantitative rt-pcr after laser-assisted cell picking. *Nat Med* 1998;4(11):1329-1333.

54. Yu H, Konigshoff M, Jayachandran A, Handley D, Seeger W, Kaminski N, Eickelberg O. Transgelin is a direct target of tgf-{beta}/smad3-dependent epithelial cell migration in lung fibrosis. *FASEB J* 2008.

55. Pardo A, Gibson K, Cisneros J, Richards TJ, Yang Y, Becerril C, Yousem S, Herrera I, Ruiz V, Selman M, et al. Up-regulation and profibrotic role of osteopontin in human idiopathic pulmonary fibrosis. *PLoS Med* 2005;2(9):e251.

56. Selman M, Pardo A, Barrera L, Estrada A, Watson SR, Wilson K, Aziz N, Kaminski N, Zlotnik A. Gene expression profiles distinguish idiopathic pulmonary fibrosis from hypersensitivity pneumonitis. *AJRCCM* 2006;173(2):188-198.

57. Kim KH, Burkhart K, Chen P, Frevert CW, Randolph-Habecker J, Hackman RC, Soloway PD, Madtes DK. Tissue inhibitor of metalloproteinase-1 deficiency amplifies acute lung injury in bleomycin-exposed mice. *AJRCMB* 2005;33(3):271-279.

58. Yang IV, Burch LH, Steele MP, Savov JD, Hollingsworth JW, McElvania-Tekippe E, Berman KG, Speer MC, Sporn TA, Brown KK, et al. Gene expression profiling of familial and sporadic interstitial pneumonia. *AJRCCM* 2007;175(1):45-54.

59. Lazar MH, Christensen PJ, Du M, Yu B, Subbotina NM, Hanson KE, Hansen JM, White ES, Simon RH, Sisson TH. Plasminogen activator inhibitor-1 impairs alveolar epithelial repair by binding to vitronectin. *AJRCMB* 2004;31(6):672-678.

60. Yeger H, Perbal B. The ccn family of genes: A perspective on ccn biology and therapeutic potential. *J Cell Comm Signal* 2007;1(3-4):159-164.

61. Brigstock DR. The ccn family: A new stimulus package. *J Endocrinol* 2003;178(2):169-175.

62. Logan CY, Nusse R. The wnt signaling pathway in development and disease. *Annu Rev Cell Dev Biol* 2004;20:781-810.

63. Moon RT, Kohn AD, De Ferrari GV, Kaykas A. Wnt and beta-catenin signalling: Diseases and therapies. *Nat Rev Genet* 2004;5(9):691-701.

64. Chen CC, Lau LF. Functions and mechanisms of action of ccn matricellular proteins. *Int J Biochem Cell Biol* 2009;41(4):771-783.

65. Leask A, Abraham DJ. All in the ccn family: Essential matricellular signaling modulators emerge from the bunker. *J Cell Sci* 2006;119(Pt 23):4803-4810.

66. Takigawa M. Ctgf/hcs24 as a multifunctional growth factor for fibroblasts, chondrocytes and vascular endothelial cells. *Drug News Perspect* 2003;16(1):11-21.

67. Kalluri R, Neilson EG. Epithelial-mesenchymal transition and its implications for fibrosis. *J Clin Invest* 2003;112(12):1776-1784.

68. Willis BC, Borok Z. Tgf-beta-induced emt: Mechanisms and implications for fibrotic lung disease. *AJP* 2007;293(3):L525-534.

69. Gross TJ, Hunninghake GW. Idiopathic pulmonary fibrosis. *N Engl J Med* 2001;345(7):517-525.

70. Strieter RM. Mechanisms of pulmonary fibrosis: Conference summary. *Chest* 2001;120(1 Suppl):77S-85S.

71. Gauldie J, Kolb M, Sime PJ. A new direction in the pathogenesis of idiopathic pulmonary fibrosis? *Respir Res* 2002;3(1):1.

72. Chapman HA. Disorders of lung matrix remodeling. *J Clin Invest* 2004;113(2):148-157.

73. Kuhn C, 3rd, Boldt J, King TE, Jr., Crouch E, Vartio T, McDonald JA. An immunohistochemical study of architectural remodeling and connective tissue synthesis in pulmonary fibrosis. *Am Rev Respir Dis* 1989;140(6):1693-1703.

74. Haschek WM, Witschi H. Pulmonary fibrosis--a possible mechanism. *Toxicol Appl Pharmacol* 1979;51(3):475-487.

75. Lee CG, Kang HR, Homer RJ, Chupp G, Elias JA. Transgenic modeling of transforming growth factor-beta(1): Role of apoptosis in fibrosis and alveolar remodeling. *Proc Am Thorac Soc* 2006;3(5):418-423.

76. Lee CG, Cho SJ, Kang MJ, Chapoval SP, Lee PJ, Noble PW, Yehualaeshet T, Lu B, Flavell RA, Milbrandt J, et al. Early growth

response gene 1-mediated apoptosis is essential for transforming growth factor beta1-induced pulmonary fibrosis. *J Exp Med* 2004;200(3):377-389.

77. Kuwano K, Hagimoto N, Kawasaki M, Yatomi T, Nakamura N, Nagata S, Suda T, Kunitake R, Maeyama T, Miyazaki H, et al. Essential roles of the fas-fas ligand pathway in the development of pulmonary fibrosis. *J Clin Invest* 1999;104(1):13-19.

78. Kuwano K, Hagimoto N, Maeyama T, Fujita M, Yoshimi M, Inoshima I, Nakashima N, Hamada N, Watanabe K, Hara N. Mitochondria-mediated apoptosis of lung epithelial cells in idiopathic interstitial pneumonias. *Lab Invest* 2002;82(12):1695-1706.

79. Uhal BD, Joshi I, Hughes WF, Ramos C, Pardo A, Selman M. Alveolar epithelial cell death adjacent to underlying myofibroblasts in advanced fibrotic human lung. *AJP* 1998;275(6 Pt 1):L1192-1199.

80. Plataki M, Koutsopoulos AV, Darivianaki K, Delides G, Siafakas NM, Bouros D. Expression of apoptotic and antiapoptotic markers in epithelial cells in idiopathic pulmonary fibrosis. *Chest* 2005;127(1):266-274.

81. Korfei M, Ruppert C, Mahavadi P, Henneke I, Markart P, Koch M, Lang G, Fink L, Bohle RM, Seeger W, et al. Epithelial endoplasmic reticulum stress and apoptosis in sporadic idiopathic pulmonary fibrosis. *AJRCCM* 2008;178(8):838-846.

82. Hagimoto N, Kuwano K, Inoshima I, Yoshimi M, Nakamura N, Fujita M, Maeyama T, Hara N. Tgf-beta 1 as an enhancer of fas-mediated apoptosis of lung epithelial cells. *J Immunol* 2002;168(12):6470-6478.

83. Thannickal VJ, Horowitz JC. Evolving concepts of apoptosis in idiopathic pulmonary fibrosis. *Proc Am Thorac Soc* 2006;3(4):350-356.

84. Adamson IY, Young L, Bowden DH. Relationship of alveolar epithelial injury and repair to the induction of pulmonary fibrosis. *Am J Path* 1988;130(2):377-383.

85. Fukuda Y, Ferrans VJ, Schoenberger CI, Rennard SI, Crystal RG. Patterns of pulmonary structural remodeling after experimental paraquat

toxicity. The morphogenesis of intraalveolar fibrosis. *Am J Path* 1985;118(3):452-475.

86. Chilosi M, Poletti V, Murer B, Lestani M, Cancellieri A, Montagna L, Piccoli P, Cangi G, Semenzato G, Doglioni C. Abnormal re-epithelialization and lung remodeling in idiopathic pulmonary fibrosis: The role of deltan-p63. *Lab Invest* 2002;82(10):1335-1345.

87. Chilosi M, Poletti V, Zamo A, Lestani M, Montagna L, Piccoli P, Pedron S, Bertaso M, Scarpa A, Murer B, et al. Aberrant wnt/beta-catenin pathway activation in idiopathic pulmonary fibrosis. *Am J Path* 2003;162(5):1495-1502.

88. Haddad R, Massaro D. Idiopathic diffuse interstitial pulmonary fibrosis (fibrosing alveolitis), atypical epithelial proliferation and lung cancer. *Am J Med* 1968;45(2):211-219.

89. Coalson JJ. The ultrastructure of human fibrosing alveolitis. *Virchows Arch A Pathol Anat Histol* 1982;395(2):181-199.

90. Corrin B, Dewar A. Pathogenesis of idiopathic interstitial pulmonary fibrosis. *Ultrastruct Pathol* 1996;20(4):369-371.

91. Brody AR, Craighead JE. Interstitial associations of cells lining air spaces in human pulmonary fibrosis. *Virchows Arch A Pathol Anat Histol* 1976;372(1):39-49.

92. Samet JM. Does idiopathic pulmonary fibrosis increase lung cancer risk? *AJRCCM* 2000;161(1):1-2.

93. Sharma OP, Lamb C. Cancer in interstitial pulmonary fibrosis and sarcoidosis. *Curr Opin Pulm Med* 2003;9(5):398-401.

94. Ma Y, Seneviratne CK, Koss M. Idiopathic pulmonary fibrosis and malignancy. *Curr Opin Pulm Med* 2001;7(5):278-282.

95. Pennica D, Swanson TA, Welsh JW, Roy MA, Lawrence DA, Lee J, Brush J, Taneyhill LA, Deuel B, Lew M, et al. Wisp genes are members of the connective tissue growth factor family that are up-regulated in wnt-1-transformed cells and aberrantly expressed in human colon tumors. *PNAS* 1998;95(25):14717-14722.

96. Selman M, Pardo A, Kaminski N. Idiopathic pulmonary fibrosis: Aberrant recapitulation of developmental programs? *PLoS Med* 2008;5(3):e62.

97. Levay-Young BK, Navre M. Growth and developmental regulation of wnt-2 (irp) gene in mesenchymal cells of fetal lung. *AJP* 1992;262(6 Pt 1):L672-683.

98. Shu W, Jiang YQ, Lu MM, Morrisey EE. Wnt7b regulates mesenchymal proliferation and vascular development in the lung. *Development* 2002;129(20):4831-4842.

99. Li C, Xiao J, Hormi K, Borok Z, Minoo P. Wnt5a participates in distal lung morphogenesis. *Dev Biol* 2002;248(1):68-81.

100. Okubo T, Hogan BL. Hyperactive wnt signaling changes the developmental potential of embryonic lung endoderm. *J Biol* 2004;3(3):11.

101. Mucenski ML, Wert SE, Nation JM, Loudy DE, Huelsken J, Birchmeier W, Morrisey EE, Whitsett JA. Beta-catenin is required for specification of proximal/distal cell fate during lung morphogenesis. *J Biol Chem* 2003;278(41):40231-40238.

102. Mucenski ML, Nation JM, Thitoff AR, Besnard V, Xu Y, Wert SE, Harada N, Taketo MM, Stahlman MT, Whitsett JA. Beta-catenin regulates differentiation of respiratory epithelial cells in vivo. *AJP* 2005;289(6):L971-979.

103. Konigshoff M, Balsara N, Pfaff EM, Kramer M, Chrobak I, Seeger W, Eickelberg O. Functional wnt signaling is increased in idiopathic pulmonary fibrosis. *PLoS ONE* 2008;3(5):e2142.

104. Morrisey EE. Wnt signaling and pulmonary fibrosis. *Am J Path* 2003;162(5):1393-1397.

105. Bilic J, Huang YL, Davidson G, Zimmermann T, Cruciat CM, Bienz M, Niehrs C. Wnt induces injuryand promotes dishevelled-dependent lrp6 phosphorylation. *Science* 2007;316(5831):1619-1622.

106. Forde JE, Dale TC. Glycogen synthase kinase 3: A key regulator of cellular fate. *Cell Mol Life Sci* 2007;64(15):1930-1944.

107. Lewis CC, Yang JY, Huang X, Banerjee SK, Blackburn MR, Baluk P, McDonald DM, Blackwell TS, Nagabhushanam V, Peters W, et al. Disease-specific gene expression profiling in multiple models of lung disease. *AJRCCM* 2008;177(4):376-387.

108. Saxena N, Banerjee S, Sengupta K, Zoubine MN, Banerjee SK. Differential expression of wisp-1 and wisp-2 genes in normal and transformed human breast cell lines. *Mol Cell Biochem* 2001;228(1-2):99-104.

109. Su F, Overholtzer M, Besser D, Levine AJ. Wisp-1 attenuates p53-mediated apoptosis in response to DNA damage through activation of the akt kinase. *Genes Dev* 2002;16(1):46-57.

110. Colston JT, de la Rosa SD, Koehler M, Gonzales K, Mestril R, Freeman GL, Bailey SR, Chandrasekar B. Wnt-induced secreted protein-1 is a prohypertrophic and profibrotic growth factor. *Am J Physiol Heart Circ Physiol* 2007;293(3):H1839-1846.

111. Chen PP, Li WJ, Wang Y, Zhao S, Li DY, Feng LY, Shi XL, Koeffler HP, Tong XJ, Xie D. Expression of cyr61, ctgf, and wisp-1 correlates with clinical features of lung cancer. *PLoS ONE* 2007;2(6):e534.

112. He B, You L, Uematsu K, Xu Z, Lee AY, Matsangou M, McCormick F, Jablons DM. A monoclonal antibody against wnt-1 induces apoptosis in human cancer cells. *Neoplasia* 2004;6(1):7-14.

113. You L, He B, Xu Z, Uematsu K, Mazieres J, Mikami I, Reguart N, Moody TW, Kitajewski J, McCormick F, et al. Inhibition of wnt-2-mediated signaling induces programmed cell death in non-small-cell lung cancer cells. *Oncogene* 2004;23(36):6170-6174.

114. Xu L, Corcoran RB, Welsh JW, Pennica D, Levine AJ. Wisp-1 is a wnt-1- and beta-catenin-responsive oncogene. *Genes Dev* 2000;14(5):585-595.

115. Zuo F, Kaminski N, Eugui E, Allard J, Yakhini Z, Ben-Dor A, Lollini L, Morris D, Kim Y, DeLustro B, et al. Gene expression analysis reveals matrilysin as a key regulator of pulmonary fibrosis in mice and humans. *PNAS* 2002;99(9):6292-6297.

116. Rosas IO, Richards TJ, Konishi K, Zhang Y, Gibson K, Lokshin AE, Lindell KO, Cisneros J, Macdonald SD, Pardo A, et al. Mmp1 and mmp7 as potential peripheral blood biomarkers in idiopathic pulmonary fibrosis. *PLoS Med* 2008;5(4):e93.

117. Berman JS, Serlin D, Li X, Whitley G, Hayes J, Rishikof DC, Ricupero DA, Liaw L, Goetschkes M, O'Regan AW. Altered bleomycin-induced lung fibrosis in osteopontin-deficient mice. *AJP* 2004;286(6):L1311-1318.

118. Agnihotri R, Crawford HC, Haro H, Matrisian LM, Havrda MC, Liaw L. Osteopontin, a novel substrate for matrix metalloproteinase-3 (stromelysin-1) and matrix metalloproteinase-7 (matrilysin). *J Biol Chem* 2001;276(30):28261-28267.

119. Brabletz T, Jung A, Dag S, Hlubek F, Kirchner T. Beta-catenin regulates the expression of the matrix metalloproteinase-7 in human colorectal cancer. *Am J Path* 1999;155(4):1033-1038.

120. Schwartz DR, Wu R, Kardia SL, Levin AM, Huang CC, Shedden KA, Kuick R, Misek DE, Hanash SM, Taylor JM, et al. Novel candidate targets of beta-catenin/t-cell factor signaling identified by gene expression profiling of ovarian endometrioid adenocarcinomas. *Cancer Res* 2003;63(11):2913-2922.

121. El-Tanani M, Platt-Higgins A, Rudland PS, Campbell FC. Ets gene pea3 cooperates with beta-catenin-lef-1 and c-jun in regulation of osteopontin transcription. *J Biol Chem* 2004;279(20):20794-20806.

122. Horowitz JC, Rogers DS, Simon RH, Sisson TH, Thannickal VJ. Plasminogen activation induced pericellular fibronectin proteolysis promotes fibroblast apoptosis. *AJRCMB* 2008;38(1):78-87.

123. Bonniaud P, Kolb M, Galt T, Robertson J, Robbins C, Stampfli M, Lavery C, Margetts PJ, Roberts AB, Gauldie J. Smad3 null mice develop airspace enlargement and are resistant to tgf-beta-mediated pulmonary fibrosis. *J Immunol* 2004;173(3):2099-2108.

124. Sandler MA, Zhang JN, Westerhausen DR, Jr., Billadello JJ. A novel protein interacts with the major transforming growth factor-beta responsive

element in the plasminogen activator inhibitor type-1 gene. *J Biol Chem* 1994;269(34):21500-21504.

125. Coker RK, Laurent GJ. Pulmonary fibrosis: Cytokines in the balance. *Eur Respir J* 1998;11(6):1218-1221.

126. Kelly M, Kolb M, Bonniaud P, Gauldie J. Re-evaluation of fibrogenic cytokines in lung fibrosis. *Curr Pharm Des* 2003;9(1):39-49.

127. Flanders KC. Smad3 as a mediator of the fibrotic response. *Int J Exp Pathol* 2004;85(2):47-64.

128. Sheppard D. Integrin-mediated activation of latent transforming growth factor beta. *Cancer metastasis reviews* 2005;24(3):395-402.

129. Moore BB, Kolodsick JE, Thannickal VJ, Cooke K, Moore TA, Hogaboam C, Wilke CA, Toews GB. Ccr2-mediated recruitment of fibrocytes to the alveolar space after fibrotic injury. *Am J Path* 2005;166(3):675-684.

Der Lebenslauf wurde aus der elektronischen Version der Arbeit entfernt.

The curriculum vitae was removed from the electronic version of the paper.

Publications

1. **Königshoff M**, Kramer M, Balsara N, Wilhelm J, Amarie OV, Jahn A, Rose F, Fink L, Seeger W, Schäfer L, Günther A, Eickelberg O. WNT1-inducible signalling protein-1 mediates pulmonary fibrosis in mice and is upregulated in humans with idiopathic pulmonary fibrosis. *J Clin Invest*. 2009 Mar 16. [Epub ahead of print]

2. Mercer PF*, Johns RH*, Scotton CJ*, Krupiczojc MA, **Königshoff M**, Howell DCJ, McAnulty RJ, Das A, Thorley AJ, Tetley TD, Eickelberg O, Chambers RC. The pulmonary epithelium is a prominent source of PAR1-inducible CCL2 in pulmonary fibrosis. *Am J Respir Crit Care Med.* 2008 Mar 1;179(5):414-25. Epub Dec 5.

3. Sevilla-Pérez J, **Königshoff M**, Kwapiszewska G, Amarie OV, Seeger W, Weissmann N, Schermuly RT, Morty RE, Eickelberg O. Shroom expression is attenuated in pulmonary arterial hypertension *Eur Resp J.* 2008 Oct;32(4):871-80. Epub June 11.

4. **Königshoff M**, Balsara N, Pfaff EM, Kramer M, Chrobak I, Seeger W, Eickelberg O.Functional Wnt signalling is increased in idiopathic pulmonary fibrosis. *PLoS ONE.* 2008 May 14;3(5):e2142.

5. Costello CM, Howell K, Cahill E, McBryan J, **Königshoff M**, Eickelberg O, Gaine S, Martin F, McLoughlin P. Lung Selective Gene Responses to Alveolar Hypoxia: Potential Role for the Bone Morphogenetic Antagonist Gremlin in Pulmonary Hypertension. *Am J Physiol Lung Cell Mol Physiol.* 2008 Aug;295(2):L272-84. Epub 2008 May 9.

6. Queisser MA, Kouri FM, **Königshoff M**, Wygrecka M, Schubert U, Eickelberg O, Preissner KT. Loss of RAGE in Pulmonary Fibrosis:Molecular Relations to Functional Changes in Pulmonary Cell Types. *Am J Respir Cell Mol Biol.* 2008 Sep;39(3):337-45. Epub 2008 Apr 17.

7. Kouri FM, Queisser MA, **Königshoff M**, Chrobak I, Preissner KT, Seeger W, Eickelberg O. Plasminogen activator inhibitor type 1 inhibits smooth muscle cell proliferation in pulmonary arterial hypertension. *Int J Biochem Cell Biol.* 2008;40(9):1872-82.Epub 2008 Feb 2.

8. Yu H, **Königshoff M**, Jayachandran A, Handley D, Seeger W, Kaminski N, Eickelberg O. Transgelin is a direct target of TGF-{beta}/Smad3-dependent epithelial cell migration in lung fibrosis. *FASEB J.* 2008 June;22(6):1778-89. Epub 2008 Feb 1.

9. Kitowska K, Zakrzewicz D, **Königshoff M**, Chrobak I, Grimminger F, Seeger W, Bulau P, Eickelberg O. Functional role and species-specific contribution of arginases in pulmonary fibrosis. *Am J Physiol Lung Cell Mol Physiol.* 2008 Jan;294(1):L34-45. Epub 2007 Oct 12.

10. **Königshoff M**, Wilhelm A, Jahn A, Sedding D, Amarie OV, Eul B, Seeger W, Fink L, Günther A, Eickelberg O, Rose F. The angiotensin II receptor 2 is expressed and mediates angiotensin II signalling in lung fibrosis. *Am J Respir Cell Mol Biol.* 2007 Dec;37(6):640-50. Epub 2007 Jul 13.

11. Vadász I, Morty RE, Olschewski A, **Königshoff M**, Kohstall MG, Ghofrani HA, Grimminger F, Seeger W. Thrombin impairs alveolar fluid clearance by promoting endocytosis of Na+,K+-ATPase. *Am J Respir Cell Mol Biol.* 2005 Oct;33(4):343-54. Epub 2005 Jul 13.

12. **Königshoff M**, Wilhelm J, Bohle RM, Pingoud A, Hahn M. HER-2/neu gene copy number quantified by real-time PCR: comparison of gene amplification, heterozygosity, and immunohistochemical status in breast cancer tissue. Clin Chem. 2003 Feb;49(2):219-29.

Manuscripts in revision or provisional accept

1. **Königshoff M**, Eickelberg O. WNT signalling in lung disease: A failure or a regeneration signal? Provisional accept by *AJRCMB.*

2. Scotton CJ*, Krupiczojc MA*, **Königshoff M**, Gary Lee YC, Kaminski N, Morser J, Post JM, Maher TM, Nicholson AG, Moffatt JD, Laurent GJ, Derian CK, Eickelberg O and Chambers RC. Local extrahepatic upregulation of coagulation factor X: potential novel role in fibrotic lung disease. in revision with *J Clin Invest.*

3. Jayachandran A, **Königshoff M**, Yu H, Rupniewska E, Hecker M, Klepetko W, Seeger W, Eickelberg O. SNAI transcription factors are key mediators of epithelial-to-mesenchymal transition in lung fibrosis. in revision with *Thorax.*

4. **Königshoff M**, Dumitrascu R, Udalov S, Amarie OV, Reiter R, Grimminger F, Seeger W, Schermuly RT, Eickelberg O. Increased expression of 5-hydroxytryptamine2A/B receptors in idiopathic pulmonary fibrosis: A rationale for therapeutic intervention. in revision with *Thorax*.

Books and Book chapters

1. **Königshoff M** et al. (2009). Biochemie. In: Prüfungswissen Physikum, Thieme Verlag, Stuttgart, ISBN: 9783131452214.

2. **Königshoff M**, Brandenburger T (2008). Biochemistry for Medical Students, 2.edition, Thieme Verlag, Stuttgart, ISBN-10: 3131364114.

3. **Königshoff M**, Wilhelm J, Hahn M (2003). HER-2/neu gene copy number quantified by real-time PCR in cell lines and breast tissue. In: Wittwer C, Hahn M, Kaul K (Eds). Rapid cycle Real-time PCR: Method and Applications, Quantification. Springer Verlag, 1. Auflage, Berlin.

Oral presentations

2008   Annual Meeting of the European Respiratory Society (ERS), Berlin, Germany. "The lung epithelium is a prominent source of Wnt ligands and inhibitors in IPF".

2008   PneumoUpdate Conference, Innsbruck, Austria. "Profibrotic action of epithelial-derived Wnt ligands and inhibitors in idiopathic pulmonary fibrosis"

2007   Meeting of the German Society of Pulmonology, Assembly Cellbiology, Munich, Germany. "WISP1: A novel regulator of idiopathic pulmonary fibrosis amenable to therapeutic intervention"

2007   American Thoracic Society (ATS) International Conference, San Francisco, USA. "Wnt-inducible protein (WISP)-1: A key regulator of alveolar epithelial cell-fibroblast crosstalk in idiopathic pulmonary fibrosis"

2007   Scientific Lung Day Graz, Austria. "WISP-1, a novel regulator of idiopathic pulmonary fibrosis, is a suitable as a therapeutic target"

2007   Keystone Symposium "Molecular Mechanisms of Fibrosis: From Bench to Bedside", Tahoe City, USA. "Wnt-inducible signalling protein (WISP)-1: A novel regulator of idiopathic pulmonary fibrosis amenable to therapeutic intervention"

2006   Annual Meeting of the European Respiratory Society (ERS), Munich, Germany. "Wnt-inducible Protein (WISP-1) is involved in Growth Regulation of Alveolar Epithelial Cells in Pulmonary Fibrosis"

2006   International Colloquium of Lung Fibrosis (ICLF), Reinhartshausen, Germany. "WISP-1 is a novel profibrotic Mediator in Lung Fibrosis"

2006   PneumoUpdate Conference, Innsbruck, Austria. "Wnt-inducible Protein (WISP-1) is a Key Regulator of Alveolar Epithelial Cell Hyperplasia in Pulmonary Fibrosis"

Poster presentations

2008   FASEB Summer Research Conference, Saxton River, USA. "Increased Expression of Ect2, a Guanine Nucleotide Exchange Factor for Rho GTPases, in Hyperplastic Alveolar Epithelial Cells in IPF" M. Königshoff, S. Becker, O. Eickelberg

2008   American Thoracic Society (ATS) International Conference, Toronto, Canada. "Inhibition of Serotonin Signalling Attenuates Lung Fibrosis" M. Königshoff, R. Dumitrascu, R. Reiter, F. Grimminger, W. Seeger, R.T. Schermuly, O. Eickelberg

2008   Lung Science Conference, European Respiratory Society (ERS), Estoril, Portugal. "Idiopathic pulmonary fibrosis exhibits increased Wnt signalling" M. Königshoff, N. Balsara, E.M. Pfaff, M. Kramer, I. Chrobak, W. Seeger, O. Eickelberg

2007   Annual Meeting of the European Respiratory Society (ERS), Munich, Germany. "Matrix-independent expression of novel markers during transdifferentiation of primary alveolar epithelial cells" M. Königshoff, J. Milosevic, A. Jayachandran, J. Sevilla-Perez, O. Eickelberg

2007   International Conference Wnt Signalling in Development and Disease, Berlin, Germany. "Wnt-inducible signalling protein (WISP)-1, a novel regulator of idiopathic pulmonary fibrosis, is a suitable therapeutic target" M. Königshoff, M. Kramer, O. Amarie, W. Seeger, O. Eickelberg

2007   American Thoracic Society (ATS) International Conference, San Francisco, USA. "Rapid loss of the alveolar epithelial cell phenotype during primary culture in a matrix-independent fashion" M. Königshoff, J. Milosevic, A. Jayachandran, J. Sevilla-Perez, O. Eickelberg

2006   APS Conference "Physiological Genomics and Proteomics of Lung Disease", Ft. Lauderdale, Florida. "WISP-1, a Novel Mediator and Therapeutic Target in Pulmonary Fibrosis". M. Königshoff, J. Wilhelm, A. Jahn, O. Amarie, K. Kitowska, A. Wilhelm, R.M. Bohle, W. Seeger, F. Rose, L. Fink, A.Guenther, O. Eickelberg.

2006   American Thoracic Society (ATS) International Conference, San Diego, USA. "CCN Cytokines are Novel Growth Regulatory Mediators of Alveolar Epithelial Cells in Lung Fibrosis". M. Königshoff, J. Wilhelm, R.M. Bohle, A. Günther, W. Seeger, F. Rose, L. Fink, O. Eickelberg.

2006	Keystone Symposia "Wnt and beta-Catenin Signalling in Development and Disease", Snowbird, USA. "Wnt-inducible Proteins Mediate Cell Growth in Pulmonary Fibrosis". M. Königshoff, J. Wilhelm, A. Jahn, O. Amarie, K. Kitowska, A. Wilhelm, R.M. Bohle, W. Seeger, F. Rose, L. Fink, A. Günther, O. Eickelberg.
2006	Annual Meeting of the German Society of Pulmonology, Nurnberg, Germany. "Funktionelle Analyse von Fibroblasten in der Bleomycin-induzierten Lungen-fibrose". M. Königshoff, A. Wilhelm, J. Kamin, A. Jahn, L. Fink, R. Bohle, W. Seeger, F. Rose.
2005	American Thoracic Society (ATS) International Conference, San Diego, USA. "Comparative characterization of bleomycin-induced lung fibrosis by volume CT, compliance measurement, and histology for gene expression analysis". M. Königshoff, A. Wilhelm, S. Greschus, C. Ruppert, K. Petri, G. Dahlem, S. Krick, R.M. Bohle, W. Seeger, A. Günther, L. Fink, F. Rose.
2005	30th Annual Conference of the Federation of European Biochemical Societies (FEBS) and 9th Conference of the International Union of Biochemsitry and Molecular Biology (IUBMB), Budapest, Hungary. "Differentially expressed genes in fibrotic alveolar epithelial cells". M. Königshoff, J. Wilhelm, W. Seeger, L. Fink, R.M. Bohle, A. Günther, F. Rose.
2005	European Union (EU)/European Molecular Biology Organization (EMBO) practical course: Advanced Techniques in Molecular Medicine, Uppsala, Sweden. "Analysis of mesenchymal-epithelial interactions in lung fibrosis". M. Königshoff, F. Rose, L. Fink, W. Seeger.

DECLARATION

I declare that I have completed this dissertation single-handedly without the unauthorized help of a second party and only with the assistance acknowledged therein. I have appropriately acknowledged and referenced all text passages that are derived literally from or are based on the content of published or unpublished work of others, and all information that relates to verbal communications. I have abided by the principles of good scientific conduct laid down in the charter of the Justus Liebig University of Giessen in carrying out the investigations described in the dissertation.

_____   _____

Place and Date   Dr. Melanie Königshoff